Xylose Metabolism in *Candida albicans*

Adam Li

A Thesis
in
The Department
of
Biology

Presented in Partial Fulfillment of the Requirements
for the Degree of Master of Science (Biology) at
Concordia University
Montreal, Quebec, Canada

April 2015

CONCORDIA UNIVERSITY

School of Graduate Studies

This is to certify that the thesis prepared

By: Adam Li

Entitled: Xylose Metabolism in *Candida albicans*

and submitted in partial fulfillment of the requirements for the degree of

Master of Science (Biology)

complies with the regulations of the University and meets the accepted standards with respect to originality and quality.

Signed by the final examining committee:

_____ Chair

Dr. Patrick Gulick

_____ Examiner

Dr. Vincent Martin

_____ Examiner

Dr. Vladimir Titorenko

_____ External Examiner

Dr. Catherine Bachewich

_____ Supervisor

Dr. Malcolm Whiteway

Approved by _____

Chair of Department or Graduate Program Director

Date: _____, 2015 _____

Dean of Faculty

ABSTRACT

Xylose Metabolism in *Candida albicans*

Adam Li

The ascomycetes *S. cerevisiae* and *C. albicans* metabolize the pentose sugar xylose differently. *S. cerevisiae* cannot grow on xylose as the sole carbon source while *C. albicans* can. In the xylose-metabolic pathway, xylose is reduced to xylitol by a xylose reductase (*GRE3*), then oxidized to xylulose by a xylose dehydrogenase (*ScSOR1*, *CaXYL2*). These two enzymes are essential for the xylose metabolic pathway. Although *S. cerevisiae* does not grow in xylose medium, it has been shown that the enzymes have enzymatic potential when used to complement various *C. albicans* knockouts. *C. albicans* was used as a model to study the function of various pairings of the reductase and dehydrogenase from the two ascomycetes. Transcription profiling confirmed the presence of *GRE3* and *XYL2* in growing strains and the absence in non-growing strains. It was found that the *CaGRE3* possessed an N-terminal extension that improved the functioning of heterologous *GRE3/SOR1* combinations. Metabolite analysis showed increased import of xylose when subject to xylose adaption compared to unadapted strains. *C. albicans* is able to use glucogenic amino acids as a source of carbon, with or without the presence of xylose enzymes. Overall, this work establishes the enzymatic interactions between the xylose reductase and xylose dehydrogenase in *S. cerevisiae* and *C. albicans*, as well as their effects on the cell.

Acknowledgements

First and foremost, I want to thank my supervisor Dr. Malcolm Whiteway for his continuous guidance, support and patience, as well as for the collaborative research environment he has created. It is an honor for me to have worked with him and to be his first Master's student registered at Concordia University.

I would like to thank Dr. Dajana Vuckovic and her team for the metabolite analysis of my strains. A lot of work was put to troubleshoot the experiments and I thank them for their patience.

I would like to thank Dr. Vincent Martin and Dr. Vladimir Titorenko for taking part on my committee, as well as Dr. Catherine Bachewich as an external examiner.

Thank you to all of the lab members (past and present) for their support and for being a good group of friends with such diverse personalities. Special thanks to Daniel Dignard and Doreen Harcus for constructing the deletion and complementation strains. Special thanks to former lab member Dr. Jaideep Mallick for sharing his knowledge and expert advice.

I would like to thank BioFuelNet and NSERC for funding this project and giving me the opportunity to take part of their annual BioFuelNet Symposiums.

Contribution of Authors

I would like to thank Dr. Dajana Vuckovic and her team (Dmitri, Parsram, Mathilde) who are part of the Centre for Biological Applications of Mass Spectrometry, for helping me perform the liquid-chromatography mass spectrometry necessary for my metabolite analysis data.

Table of Contents

List of Figures

List of Tables

List of Abbreviations

Ca	*Candida albicans*
Cy	Cyanine
G6P	Glucose-6-Phosphate
HILIC	HydrophILic Interaction Chromatography
HPLC	High-Performance Liquid Chromatography
LB	Luria-Bertani
LC-MS	Liquid Chromatography–Mass Spectrometry
LTQ	Linear Trap Quadropole
OD	Optical Density
NAD	Nicotinamide Adenine Dinucleotide
NADP	Nicotinamide Adenine Dinucleotide Phosphate
PCR	Polymerase Chain Reaction
PPP	Pentose Phosphate Pathway
SC	Synthetic Complete
Sc	*Saccharomyces cerevisiae*
SX	Synthetic complete with filter sterilized Xylose
TCA	TriCarboxylic Acid
URA3	URAcil auxotrophic marker
WT	Wild Type
XDH	Xylose DeHydrogenase
XR	Xylose Reductase
YNB	Yeast Nitrogen Base
YPD	Yeast Peptone Dextrose

Introduction

Candida albicans is a commensal human fungus that is a common component of mucosal surfaces and of the gastrointestinal tract (Beck-Sagué & Jarvis, 1993) . It is an opportunistic pathogen, and can be a significant threat for immunocompromised people (Beck-Sagué & Jarvis, 1993; Klein et al., 1984). The treatment of *C. albicans* infections is estimated to cost at least $1 billion annually in North America (Miller, Hajjeh, & Edwards, 2001), and it is identified to be the fourth most common nosocomial infection in US hospitals. C. *albicans* has the ability to grow in unicellular yeast, pseudohyphal and hyphal forms, which makes the pathogen's life cycle and biology interesting (Beck-Sagué & Jarvis, 1993; Sudbery, Gow, & Berman, 2004). The ability to grow in different cellular forms is considered to be a component of the organism's repertoire that makes it a successful commensal and pathogen, because different forms can be useful in exploiting different niches within the human body.

Differential carbon source utilization can also aid this opportunistic pathogen in its ability to exploit different niches. It has been shown that *C. albicans* uses different carbon metabolic pathways at different stages of an infection, an approach that might be crucial for the establishment of the invasive disease (Barelle et al., 2006; Beck-Sagué & Jarvis, 1993; Klein et al., 1984). In the early stages of infection, *C. albicans* upregulates the glyoxylate and gluconeogenic pathways, after phagocytosis by neutrophils and macrophages, where glucose is in relatively short supply (Lorenz, Bender, & Fink, 2004; Miller et al., 2001). However, in the later stages of infection, when *C. albicans* colonizes internal organs such as the kidney, which is glucose-rich, the glycolytic pathway predominates (Barelle et al., 2006). Mutations in each of these central metabolic pathways attenuate the virulence of *C. albicans*, suggesting that the three pathways are

necessary for the establishment of a systemic infection. *C. albicans* can also undergo phenotypic transitions between forms designated as white and opaque (Huang, 2012). It has been shown that white cells express a fermentative profile of metabolism related genes, while opaque cells adopt an oxidative one (Lan et al., 2002). It has been suggested that that the niche-specific regulation of carbon metabolism increases the biological fitness of *C. albicans* within its host (Barelle et al., 2006).

In the model yeast *S. cerevisiae*, growth in glucose as the sole carbon source represses the transcription of numerous genes in alternative carbon pathways, a process termed glucose repression (Carlson, 1999). Yeast grown with an alternative carbon source (i.e. galactose or glycerol) undergoes catabolite de-repression. During catabolite de-repression, yeast metabolism shifts from fermentation to respiration and carbon is directed to the TCA cycle, hence increasing electron transport and respiration (Lin et al., 2002). During catabolite de-repression, there is an increased gene expression in yeast amino acid permeases, amino acid uptake and oxygen consumption (Peter, Düring, & Ahmed, 2006). It has been shown that *C. albicans* can utilize amino acids as a source of energy, without the presence of any sugar (Lorenz, 2013). When *S. cerevisiae* undergoes carbon catabolite de-repression, intracellular transport of L-arginine and L-leucine increases by 10-25 fold (Peter et al., 2006). For example, L-leucine is a common intermediate of major catabolic pathways such as acetyl-CoA, pyruvate or 2-oxoglutarate (Hothersall & Ahmed, 2013).

The baker's yeast *S. cerevisiae* lineage is consistent with the universal genetic code in that it uses the codon CTG to encode leucine, whereas the fungal pathogen *C. albicans* encodes CTG for serine. These ascomycetes have diverse ecological niches. *S.*

cerevisiae is a nomadic yeast with no niche, whereas *C. albicans* is a human commensal pathogen that resides on mucosal surfaces in the gastrointestinal system (Bezerra et al., 2013; Goddard & Greig, 2015). These different niches can be exploited by adaptations permitting cells to live in different environments. For example, baker's yeast is limited to metabolizing 6-carbon sugars whereas the fungal pathogen can grow on xylose and adapt to various stressful environments (A. J. P. Brown et al., 2014b). For example, upon internalization by macrophages, the fungal pathogen utilizes the amino acids of immune cell for conversion into either acetyl-CoA or TCA intermediates, which would eventually be fluxed into the gluconeogenic pathway.

The commonly used yeast for biofuel production, *Saccharomyces cerevisiae,* is unable to utilize pentose sugars, which includes a considerable portion of lignocellulosic biomass (Matsushika, Inoue, Kodaki, & Sawayama, 2009). Glucose (60-70%) and xylose (30-40%) are the most abundant sugars in cellulosic hydrolysates and are abundant in the biosphere (Mosier et al., 2005), and these could be a source of renewable liquid fuels. Ideally, it would be best to use sugars that we don't eat for ethanol fermentation, so efficient and rapid utilization of xylose would be a important component of producing biofuels and chemicals from renewable biomass, sustainably and economically (Somerville, 2007). The ability to improve xylose catabolism and conversion in a recombinant host such as *S. cerevisiae* would increase the potential of improving biofuels and biochemical production. Bioethanol is being produced from starchy biomass, corn food as raw material, wheat starch and cane sugars, which could consequently create a competition between food and fuel. While *S. cerevisiae* cannot metabolize xylose, it can utilize xylulose as the sole carbon source, suggesting that *S. cerevisiae* lacks the

enzymatic capacity to convert xylose to xylulose (Deng & Ho, 1990). Although *S. cerevisiae* cannot grow on or ferment xylose, it was found that *S. cerevisiae*, *S. pombe* and other yeasts were able to ferment xylulose. Other yeast strains such as *P. tannophilus* and *S. stipitis*, have been reported to ferment xylose into ethanol but the rate and yield of these xylose-utilizing strains were considerably less compared to their glucose fermentation (Slininger, Bothast, Van Cauwenberge, & Kurtzman, 1982). Microbial strain development through the requirement of economic fermentation of pentose sugars to ethanol has been a very active field. Genetic engineering and adaptation may be potential methods to develop sufficient xylose fermentation in *S. cerevisiae*.

The first determining step in xylose catabolism is the transport of xylose into the cell (Young, Poucher, Comer, Bailey, & Alper, 2011). In *S. cerevisiae*, xylose is transported by members of the HXT family of hexose transporters which have a much higher affinity for glucose when compared to xylose (Saloheimo et al., 2007). Once xylose is transported into the cell, one of two main assimilation pathways can be utilized (Young, Lee, & Alper, 2010). In yeasts, filamentous fungi and other eukaryotes, this proceeds via a two-step reduction and oxidation through the heterologous expression of a xylose reductase (XR) and a xylitol dehydrogenase (XDH)(Figure 1) (Hahn-Hägerdal, Karhumaa, Jeppsson, & Gorwa-Grauslund, 2007). However, studies have shown that this pathway is limited from a cofactor imbalance with the reductase utilizing NADPH while the dehydrogenase utilizes NAD+, which can lead to a decrease in ethanol yield (Young et al., 2010). This disparity could be due to competition for NAD+ by other endogenous metabolic enzymes or to inefficient xylose pathway enzymes. In bacteria, an alternative pathway for xylose catabolism exists (Figure 1). This consist of an isomerase-based

pathway which does not require any cofactors (Brat, Boles, & Wiedemann, 2009). Studies have shown successful expression of xylose isomerase genes from *Piromyces sp. and Orpinomyces sp.* in *S. cerevisiae* which improved the knowledge of efficient xylose fermentation (Madhavan et al., 2009).

The related ascomycete, *Candida albicans,* is able to grow on xylose but is unable to ferment xylose to ethanol. *S. cerevisiae* and *C. albicans* contain highly similar genes that encode the XR and XDH genes. It has been reported that the xylose utilization of a *C. albicans* strain deleted for its XR/XDH genes can be complemented by the *S. cerevisiae* XR/XDH genes (Harcus et al., 2013). This rescued strain, called CA271, is able to utilize xylose but with very weak ability compared to the wild type or either singly complemented strains. It has been suggested that the *S. cerevisiae* XR/XDH proteins may not be perfectly connected to the other parts of the metabolic pathways of *C. albicans*, as saturated growth of CA271 on xylose takes three weeks (Figure 2A, 2B). It appears the proper coupling of all the steps in the xylose metabolic pathway is as important as the enzyme activities.

A sequence alignment of the xylose reductases of the fungal kingdom showed that the *C. albicans GRE3* ,which functions to metabolize xylose, had an N-terminal sequence motif extension compared to the reductases of other yeasts (Figure 3). We wanted to investigate whether this N-terminal extension posed an advantage to the *GRE3* enzymatic function, since it has been shown that sugar transport preference and kinetics can be rewired through the insertion of a specific sequence motif (Young, Tong, Bui, Spofford, & Alper, 2014).

Metabolomics is the study of global changes in the entire metabolome in a single organism. Its workflow consists of metabolite sample extraction, quenching, extraction and the analysis of metabolites using analytical or statistical tools (Ryan & Robards, 2006). Metabolomics has been suggested as a more rational and systematic approach for strain improvements by identification of target metabolites (van der Werf, Jellema, & Hankemeier, 2005). In the first step of utilizing exogenous sugars, the molecular transport of xylose into the cell can serve as a significant flux bottleneck (Young et al., 2014). Here, we use metabolite analysis to determine the differences in xylose uptake, intracellular concentrations and metabolism that result from the different combinations of xylose reductase and dehydrogenase.

We report the metabolic engineering of the xylose reductase gene in CA271 for improved cell growth. Metabolic engineering is a candidate approach for tailoring proteins that require refined functions (such as higher stability, substrate specificity, product selectivity of protein). We also investigated metabolic adaption as well as metabolic engineering using selection for increased cell growth on xylose as a sole carbon source to investigate what makes the XR/XDH module in *C. albicans* work compared to that of *S. cerevisiae.* We also report the difference between *C. albicans* and *S. cerevisiae*, of which the fungal pathogen can shift its metabolism in response to new environments, such as being able to grow in a glucogenic amino acid environment.

Materials and Methods

Strains and Culture Conditions

The *C. albicans* strains used in this study are listed in Table 3. Strain SC5314 is a clinical isolate, mutants *gre3, xyl2* and *gre3/xyl2* were constructed from parent strain SN148 (Harcus et al., 2013). CDH139, CA256 and CA271 were constructed by complementing the mutant strains with either *ScGRE3* and/or *ScSOR1* using the CIpACT1-CYC vector (Harcus et al., 2013). CA271 Adapted strains were created by growing CA271 on a xylose medium prior to liquid growth. AL001 was created by integrating pAL001 digested with *Mlu*I and the N-terminus of *CaGRE3* to create the *CaScGRE3* gene through homologous recombination. AL002 and AL003 were created by complementing *gre3* and CA270 with pAL003. Wild type and *gre3/xyl2* used as baselines when assaying growth curves.

Candida albicans and *Saccharomyces cerevisiae* yeast strains were grown at 30^{o}C in yeast peptone dextrose (YPD) or synthetic complete (SC)(0.67% Difco yeast nitrogen base with amino acids) with filter sterilized D-xylose (SX)(2%), all supplemented with adenine and uridine. *E. coli* strain DH5*α* grown at 37^{o}C in Lysogeny-Broth (LB) broth with 225 RPM orbital shaking and was used for all cloning and plasmid propagation. Yeast and bacterial strains were stored at -80^{o}C in 20% glycerol.

Growth Curves

Overnight cell cultures were grown in YPD medium containing dextrose (2%). Cells were washed three times with two volumes of the starting-culture-volume of sterile water before diluting to an OD660 nm of 0.2 in 5-10 ml of synthetic complete medium

containing xylose (2%). Cells were grown aerobically at 30^{o}C with 225 RPM orbital shaking, and the OD660 nm was taken at intervals for up to two weeks.

When doing growth curves in 50mL falcon tubes (for strains requiring more than a five days to grow), a spectrophotometer was used to measure optical density. Cells were diluted to an OD660nm of 0.1 in 10mL of media. Cells were grown aerobically at 30^{o}C with 220 RPM orbital shaking, and the OD660nm was taken at daily intervals. When doing growth curves in 96-well plates (for strains that require five days or less to grow), the TECAN Sunrise machines were used. In these experiments, cells were diluted to an OD660nm of 0.1 in 200uL of media. Cells were grown aerobically at 30^{o}C with 200 RPM orbital shaking at every ten-minute-interval, and the OD660nm was taken at 10-minute intervals for five days.

Microarray Analysis

The strains SC5314, *gre3/xyl2* and CA271 of *C. albicans* were used for transcription profiling in xylose medium. A 10mL starting culture in 2% YPD was grown overnight. The cells were then washed three times with 20mL sterile water. The cell pellet was suspended in 20mL of water and was used to inoculate 50mL culture in 2% xylose at a starting OD600 of 0.1. These cultures were incubated until an increase in OD600 was observed to approximately 0.6 – 0.8. For the *gre3/xyl2* strain, the starting OD600 used was 0.8, since there was no increase in the OD600 for that strain in xylose medium.

Cells were disrupted with glass beads in the FastPrep®-24 instrument (MP Biomedicals). RNA was extracted using the RNeasy® Kit (QIAGENTM), and 20 ug of

total RNA was used for the cDNA synthesis with either cyanine-3 or cyanine-5 dyes. Probe synthesis, microarray hybridizations, washings and analyses were as described (Nantel, Rigby, & Hogues, 2006). *C. albicans* microarrays (double-spotted 6,394 intragenic 70-mer oligonucleotides) were obtained from the Biotechnology Research Institute Microarray Facility Center. To obtain the gene list, the median of ratios (which shows the intensity of color, 635nm/532nm or vice-versa, depending which strain was going to be compared to) was taken for each gene. Since duplicates were performed, the average of the median of ratios was calculated for each gene. It is these ratios that determine the difference in expression between two strains.

Protein Engineering of *GRE3*

Plasmids and oligonucleotides in this study are listed in Table 1 and 2. Two plasmids were used for this construction: CIpACT1-CYC which contains the *C. albicans ACT1* promoter, *CYC1* terminator and *RPS1* gene, to allow the cloned gene of interest to be integrated at the *RPS1* locus and expressed under the control of the *ACT1* promoter, and pRS314 which contains the *CEN/ARS* sequence and *ScGRE3* that was previously cloned between the *Mlu*I/*Nhe*I sites of CIpACT1-CYC to produce pl396 (Harcus et al., 2013). That plasmid was digested with *Kpn*I/*Spe*I and the fragment that contained *ScGRE3* was ligated into the sites of *Kpn*I/*Spe*I of pRS314 to produce pAL001 (Figure 6A, lane 6). The coding region for the N-terminal part of *CaGRE3* was amplified by PCR from *C. albicans* (SC5314) genomic DNA with primers OAL001/002 with homology with the *ACT1* promoter before the *CaGRE3* N-terminal and homology with the N-terminal region of *ScGRE3* after the *CaGRE3* N-terminus. The *CaGRE3* PCR fragment

and pAL001 (linearized with a *Mlu*I digest) were transformed into *S. cerevisiae* strain W303-1A to induce homologous recombination between ACT1p and the N-terminal of *ScGRE3* to produce pAL002 (Figure 6A, lane 9). The plasmid pAL002 was digested with *Kpn*I/*Spe*I once again and the fragment containing the fusion gene was cloned at the *Kpn*I/*Spe*I sites of CIp-ACT1-CYC to produce pAL003 (Figure 6A, lane 11). The new plasmid was linearized with a *Stu*I digest and transformed into *C. albicans gre3* and CA270 carrying the *CaScGRE3* genes to create AL001 and AL002, respectively. The genomic DNA of these strains was isolated to perform PCR to confirm integrity of the homologous recombination with primers OAL003/004, which are specific to *CaGRE3* and *ScGRE3*, and products were sent for sequencing at Genome Quebec (Submission #165761, sequenced on June 18th, 2014).

Standards for metabolite analysis

Standards of xylose, xylitol and xylulose at >99% purity were purchased from Sigma-Aldrich (St. Louis, MO). Water and Acetonitrile of LC-MS grade were purchased from Fisher Scientific (Ottawa, Canada). Ammonium acetate of HPLC grade was obtained from Merck (Darmstadt, Germany).

Sample preparation

A standard sample containing 500 ng/ml of carbohydrates (xylose, xylulose and xylitol) was freshly prepared in 95:5 of acetonitrile/water (v/v). Calibration solutions were obtained by successive dilutions of the standard sample to final concentrations of 250, 125, 62.5, 31.3 and 15.5 ng/ml. Overnight cultures were grown in YPD, washed and

grown in SX media until saturation. The cultures were washed with water to exclude any extracellular metabolites. Cells were suspended in cold 1:1 acetonitrile/water, vortexed for cell lysis, followed by centrifugation. The supernatant was extracted and suspended in cold 1:1 acetonitrile/water. The resulting extract was diluted 1:2 with 95:5 of acetonitrile/water 2 mM ammonium acetate and centrifuged for 5 min at 13,000 RPM prior to LC-MS injection. One set of spiked samples containing 250 ng/ml of each carbohydrate was also prepared to estimate degree of ionization suppression across the different extracts.

HILIC separation of carbohydrates and detection by mass spectrometry

A HP 1100 HPLC system (Agilent Technologies, Mississauga, Canada) was used for the analysis of carbohydrates. Separations were performed using an Ascentis Express HILIC 2.7 µm (100 cm × 2.1 mm) column (Sigma-Aldrich, St. Louis, MO) at a flow rate of 300 µL/min. Injections of 10 µL of samples were made onto the column. Carbohydrates were eluted using a mobile phase gradient in solvent A [95:5 of acetonitrile/water 2 mM ammonium acetate] and solvent B [60:40 of acetonitrile/water 2 mM ammonium acetate] as follows: 0–2 min, 100% A, 2-14 min linear gradient to 35% A, 14-18 min, isocratic hold at 35% A, 18-18.10 min, linear gradient to 100% A, and 18.10-30 min, column re-equilibration to 100% A.

A Thermo Fisher Scientific Velos LTQ Orbitrap high-resolution mass spectrometer (Thermo Fisher Scientific, Bremen, Germany) was used for the acquisition of the MS data in negative electrospray ionization (ESI) mode. The mass spectra were recorded over a scan range of 100−1000 Da at a resolution of R = 100,000. Instrumental

settings were as follows: sheath and auxiliary gas flow rates 30 and 10, respectively; spray voltage 3.0 kV, capillary temperature 350 °C. LC-MS data analyses were performed using Thermo Scientific Xcalibur 2.1 software supplied by the manufacturer. The amount of xylose, xylulose and xylitol was determined using MS1 extracted ion chromatograms of m/z 149.0455 and 151.0612 using external standard calibration method and 10 ppm extraction window.

Results

In fungi, the metabolism of xylose involves the conversion to xylulose in a two-step process. First, xylose is reduced to xylulose by a xylose reductase (XR), second, xylitol is oxidized to xylulose by a xylose dehydrogenase (XDH) (Figure 1). It has been shown by Harcus *et al*. that *C. albicans* mutant strains *gre3, xyl2, gre3/xyl2* did not grow on media supplemented only with xylose as a carbon source. When complemented with *ScGRE3, ScSOR1 and ScGRE3/ScSOR1* respectively, the ability to grow in xylose medium is restored. However, the growth phenotype is not rescued to that of the wild type *C. albicans*. It was observed that it takes the complemented *gre3* (CA256) three to four days to grow, the complemented *xyl2* (CDH139) seven to eight days to grow and the double complemented *gre3/xyl2* (CA271) about twenty-one to twenty-four days to grow, while the wild type strain reaches saturation after only 2 days (Figure 2A, 2B). All of the complemented strains as well as the *gre3* mutant were able to grow on xylitol after one to two days (Figure 2D), suggesting that the XDH from both *S. cerevisiae* and *C. albicans* can metabolize xylitol but when coupled with the XR to metabolize xylose, a variable lag period appears in the complemented strains (Figure 2B). We were interested in the differences in the xylose enzymes in *C. albicans* and *S. cerevisiae* that cause these distinctions.

Transcription profiling of cellular response to xylose

Previous work as established that in response to the presence of xylose, *S. cerevisiae* does not induce the genes for XR and XDH, but does induce the sugar transporter encoding genes *HXT4*, *HXT6* and *HXT7* (Harcus et al., 2013), even though the

strain shows no growth under these conditions. We have examined the response to xylose of *C. albicans* wild type, *gre3/xyl2* and CA271 through incubation of the cells with xylose as the sole carbon source. In Figure 4A, wild type is compared to *gre3/xyl2* in xylose growth conditions. Thirty eight genes have at least a 2-fold transcription increase in xylose when compared to the null mutant, and 10 of these genes have more than a 10-fold increase. The differentially expressed genes include *GRE3* and *XYL2*, due to the fact that the wild type has the XR and XDH while the null mutant does not, confirming the detection capacity of the microarrays. Several genes encoding glycolytic enzymes and sugar transporters (*HGT19, HGT20*) are also up-regulated, these are different sugar transporters compared to the profiling done by Harcus *et* al.. Other notable genes that were highly up-regulated are *LDG3* (243 fold) and *INO1* (18 fold) genes. This shows the baseline between cells that grow in xylose, versus cells that cannot. When comparing CA271 to *gre3/xyl2*, it was observed that 75 genes had at least a 4-fold transcription increase in CA271 when incubated in xylose, of which 8 genes had more than a 10-fold induction (Figure 4B). One of the induced genes included *GRE3* (103 fold), but not *XYL2*. When the DNA sequence of *CaGRE3* and *ScGRE3* were aligned using BLAST, the sequence identity showed a high sequence identity (E-value) of 5.9×10^{-54}, compared to the DNA sequence identity between *CaXYL2* and *ScSOR1*, which was considerably lower with an E value of 2.7×10^{-14}. This supports the idea that the *C. albicans* microarray chip can detect *ScGRE3* but not *ScSOR1*. Notable genes that were highly up-regulated were *LDG3* (23 fold) and *INO1* (16 fold). When comparing wild type to CA271, it was observed that only 9 genes had at least 4-fold transcription induction in the wild type when incubated in xylose, of which 4 genes had more than a 10-fold induction

(Figure 4C). One of the induced genes includes *XYL2* (95 fold), but not *GRE3* (no change in expression). This could arise because both *CaGRE3* and *ScGRE3* could be detected from the *C. albicans* microarray chip but not *ScSOR1*. As a result, since only *CaXYL2* is detected, it appears highly induced in the wild type. One of the notable genes *INO1* (16 fold) was induced once again. The other notable genes *LDG3*, that was induced when comparing either the wild type or CA271 to *gre3/xyl2*, had no change in expression, suggesting that *LDG3* is induced when cells are in good conditions of growth.

Identification of Adapted CA271 Mutants

It has been proposed that *C. albicans* has certain traits that allow it to adapt and grow in its new niches compared to a non-pathogenic yeast like *S. cerevisiae*. It has been proposed that metabolic adaptation impacts *C. albicans* pathogenicity and immunogenicity at multiple levels (A. J. P. Brown, Brown, Netea, & Gow, 2014a). I asked whether CA271 mutants could be generated that would show improved growth when streaked on 2% xylose plates. The goal was to obtain CA271 colonies that had undergone spontaneous genetic mutations to improve growth that could possibly map to either the heterologous XR or XDH genes. When *gre3/xyl2* and CA271 were grown on xylose plates for six days, colonies were observed for both strains (Figure 5A). This was unexpected because the *gre3/xyl2* mutations were non-revertable deletions, but it was possible that the *gre3/xyl2* strain was exploiting alternative carbon sources in either the YNB or the agarose. We wanted to understand this phenomenon so colonies were picked and inoculated in 2% xylose media; 36 *gre3/xyl2* revertant colonies and 60 CA271 revertant colonies from the xylose plate were picked and assessed. It was observed that

none of the *gre3/xyl2* revertants grew in liquid xylose media while all of the CA271 colonies grew to saturation (Figure 5B), suggesting that although the two strains generated similar numbers of colonies, these colonies were arising from distinct events in the two strain backgrounds. The CA271 colonies were termed "adapted" because they had an improved ability to grow in liquid medium with xylose as the sole sugar source. To further investigate the properties of these CA271 derived colonies, an adapted-evolution growth assay was performed to determine whether the xylose growing CA271 strains had undergone either genetic (stable) or physiological (transient) changes. The double complemented strain was subjected to three different environments before being assessed in xylose media: first, CA271 was streaked on a YPD plate; second, CA271 was streaked on a SX plate; third, CA271 was streaked on a SX plate, then replica plates on a YPD plate; colonies from these three scenarios were assessed in xylose media (Supplementary 5). Our hypothesis was that the first and third scenario would arrive at the same outcome, as their final environment comes from glucose. We predicted the second environment to show the most growth on xylose as it had the chance to adapt. It was observed that the second and third scenarios showed improved growth compared to the first scenario (Supplementary 6). It was observed that in the third scenario, when the adapted CA271 strains were grown on YPD, they did not de-adapt, suggesting that this adaption was not physiological, and growing CA271 on a SX plate gave *C. albicans* the inherited ability to grow in a new environment To investigate whether there were any genetic changes within the XR/XDH of the adapted CA271 strains, these genes were sequenced; there were no genetic changes suggesting that xylose adaptation may be altering the genome outside of the XR/XDH genes.

Assessing the Role of the N-terminus of *CaGRE3*

The XR/XDH module of *C. albicans* permits the fungal pathogen to efficiently metabolize xylose as a sole carbon source. However, the XR/XDH module of *S. cerevisiae,* when introduced into *C. albicans*, functions poorly compared to the endogenous *C. albicans* module and the single complemented strains. This could be due to protein stability, localization and/or expression levels. Comparative genomic studies have shown that the XR and XDH genes from *S. cerevisiae* are well conserved when compared to the orthologs in xylose metabolizing fungi such as *C. albicans.* Since the genes are structurally well conserved, we asked the question why the combined XR/XDH enzymes of *S. cerevisiae* are functioning so poorly within the heterologous host. Alignment of xylose reductase showed that the N-terminus of *C. albicans* Gre3p has a unique 55 amino acid extension that is missing in *S. cerevisiae* Gre3p. Compared to other fungal orthologs of *GRE3*, the *C. albicans* Gre3p has the largest N-terminal extension (Figure 3). To investigate this N-terminal extension, we fused this N-terminal region of the *C. albicans GRE3* to the N-terminus of the *S. cerevisiae GRE3,* and expressed this hybrid enzyme in *C. albicans*. The *GRE3* fusion protein was constructed by using restriction enzyme sites and the homologous recombination machinery in yeast. The engineered *CaScGRE3* gene contained no CTG codons. When complementing CA270 with *CaScGRE3* at the *RPS1* locus, there was a 50% probability that the *CaScGRE3* gene integration would incorporate at the correct diploid locus; alternatively the integration would replace the existing ScSOR1 integration at the other *RPS1* locus (Figure 6C). PCR was performed on genomic DNA of AL003 transformants to confirm the presence of *CaScGRE3* and *ScSOR1*. Successful transformants had both the xylose genes integrated

at the *RPS1* locus while unsuccessful transformants showed the presence of *CaScGRE3* but not *ScSOR1* (Figure 6D). When *C. albicans* strains *gre3* and CA270 were complemented with the chimeric *CaScGRE3*, it was observed that their growth was significantly improved in xylose medium compared to the strains without the chimeric Gre3p, CA256 and CA271, respectively (Figure 6E). The growth of AL002 relative to CA256 was improved by 4 fold and the growth of AL003 relative to CA271 was improved by 23 fold. To examine how the engineered XR could be significantly improving growth in *C. albicans*, a 3D model of *Candida tenuis* GRE3p was closely looked at using the program JMol. It was observed that the active site of GRE3p resides in the center of the TIM barrel, distant from the N-terminus. Since the modified N-terminus is on the opposite side from the active site, it is unlikely that the modification is increasing the catalytic function of the enzyme; it could be that the chimeric *GRE3* is interacting better with the XDH, improving the function of the XR/XDH module.

Metabolite analysis of Wild Type, CA271 and Adapted Strains

To understand the way different *C. albicans* strains metabolize xylose, metabolite analysis was performed to observe a physiological-snapshot of the cell during xylose metabolism during the logarithmic phase of cell growth. The metabolite analysis of *C. albicans* strains wild type, CA271 and four CA271 adapted strains (D1, D2, D3, D4) was examined. When creating the standard curves for xylose, it was observed that D-xylose had two different mass peaks observed at two different retention times. To confirm that there was no contamination, NMR was performed on the two peaks (data not shown). It was observed that D-xylose had two isomers at a 50% proportion, α- and β-D-xylose. To

ensure reproducibility, five replicates of the WT strain were analyzed for xylose, xylitol and xylulose, there was less than 5% variability between the replicates (data not shown). Xylose samples showed 15% variability while xylitol and xylulose showed 5% variability. It was observed that WT had relatively the lowest concentrations of intracellular xylose compared to CA271 and the adapted strains (Figure 7A). This supports the idea that *CaGRE3* can metabolize xylose into xylitol relatively better than *ScGRE3*. It was found that intracellular concentration of xylitol was relatively higher in WT compared to CA271 and adapted strains, which correlates with the results with the low amounts of xylose in the wild type (Figure 7B). Intracellular xylulose was found to be relatively higher in WT compared to CA271 and adapted strains, which correlates with the results with the higher amounts of xylitol in the wild type (Figure 7B). It was also observed that the adapted strains had slightly higher amounts of intracellular xylose, xylitol and xylulose. This could support the idea that the adapted strains are able to import more xylose than the original strain.

Amino Acid Metabolism

Intriguingly, when performing xylose growth assessments for the *C. albicans* mutants defective in the xylose metabolic pathway genes, growth was observed for the mutants on the sugar free negative control (synthetic complete, no sugar)(Figure 8A). This was surprising and suggested that *C. albicans* can efficiently use some alternative carbon source in the medium; this could be amino acids. It had been shown that when *C. albicans* cells were phagocytized by macrophages, they were able to shift their metabolism from sugars to amino acids, and this allows the fungal pathogen to survive in

its sugar-limiting environment (Lorenz et al., 2004). We further investigated the method by which *C. albicans* utilizes amino acids as a carbon source. There are two types of amino acids as potential carbon sources: glucogenic and ketogenic. A glucogenic amino acid is an amino acid that can be catabolized to pyruvate, α-ketoglutarate, succinyl-CoA, fumarate or oxaloacetate, which are all possible gluconeogenic glucose precursors. This is in contrast to ketogenic amino acids, which can only be catabolized to acetyl-CoA or acetoacetate and thus can only be transformed into fatty acids or ketone bodies. Some amino acids are precursors for both carbohydrates and ketone bodies. Growth of *C. albicans* was compared in an environment where glucogenic and ketogenic amino acids were the only carbon source. It was observed that *C. albicans* can grow on glucogenic but not on ketogenic amino acids. (Figure 8B). In humans, there are thirteen amino acids that are characterized as glucogenic. Wild type *C. albicans*, *gre3/xyl2* and *S. cerevisiae* were grown on media containing a single glucogenic amino acid as a sole possible carbon source. Out of the thirteen amino acids, growth was observed on seven of the glucogenic amino acids (serine, proline, alanine, glutamate, glutamine, aspartate, asparagine). It was observed that key enzymes in the other six glucogenic amino acids in humans were not present in *C. albicans* (Supplementary 1).

Discussion

It has been shown that *S. cerevisiae* has orthologs of the xylose metabolic enzymes of xylose using yeasts such as *C. albicans*, but is not able to use them to allow *S. cerevisiae* growth in the presence of xylose as the sole carbon source. However when we complement these enzymes into a related ascomycete such as *C. albicans*, they are able to function either individually or as a pair. However when they work as a pair, they do not appear to work efficiently. We investigated the *S. cerevisiae* xylose enzymes by mutagenesis to see if we could tailor and improve their enzymatic function in *C. albicans* with the ultimate goal of also improving enzymatic function in *S. cerevisiae*. Microarray and metabolite analysis allowed us to understand how the *S. cerevisiae* xylose genes are affecting the cell in response to xylose. At the same time, we also investigated how *C. albicans* was to shift metabolic states when it is an environment with limited glucose supply. This could help us understand why *Candida* cells are pathogenic as well as how they survive in phagocytic cells to infect host cells.

Whole-genome transcription profiling was performed between wild type, *gre3/xyl2* and CA271 to understand why CA271 was not growing on par with the wild type. When comparing the wild type and *gre3/xyl2*, 38 genes have at least a 2-fold transcription increase in xylose when compared to the null mutant, the highest expressed genes included those that are critical for xylose metabolism, such as *GRE3* (302 fold) and *XYL2* (248 fold), confirming the absence of these genes in *gre3/xyl2*. Several genes encoding glycolytic enzymes and sugar transporters are also up-regulated, suggesting that either the enzymes or metabolites work through some positive feedback system to increase the expression of other metabolic genes from other pathways or transporters.

This analysis presented the baseline between cells that grow in xylose, against cells that cannot. It was observed that when comparing the wild type and CA271 against *gre3/xyl2*, there was up-regulation of *INO1* and *LDG3.* This posed an interesting question because *INO1* is used to convert glucose-6-phosphate (G6P) into myo-inositol, which is used for phosphatidylinositol biosynthesis, but there was no source of glucose in the media. *LDG3* is a putative GPI-anchored cell wall protein, suggesting that this superfamily of proteins could be associated with xylose. Microarray analysis showed the possibility of *INO1* and *LDG3* either being associated with xylose metabolism, or with cells in growing conditions.

It was found that the XR and XDH of *S. cerevisiae* have the enzymatic capacity to metabolize xylose however, *S. cerevisiae* couldn't grow on xylose as the sole carbon source. The proper coupling of *ScGRE3/SOR1* in *C. albicans* has relatively weak ability to allow growth on xylose compared to the native *CaGRE3/XYL2*. We studied the XR/XDH module of *S. cerevisiae* in *C. albicans* in two ways. The first way to improve growth on xylose was to identify spontaneous mutants through metabolic adaptation. It was observed when *gre3/xyl2* and CA271 were streaked on xylose plates, growth was observed after a lag period of six days, although we expected *gre3/xyl2* not to grow. One possibility for this is that the double mutant was exploiting an alternative carbon sources in either the YNB or the agarose. We defined the lag period as the time it takes for the strain to go through metabolic adaptation. Nonetheless, when the colonies on xylose plates were picked off and assessed in xylose media, the *gre3/xyl2* derivatives did not grow while the CA271 variants were able to grow to saturation. To confirm whether it was a physiological or genetic change, the CA271 derivatives were re-streaked on YPD

after being subjected to selection on xylose. Colonies for CA271 were once again picked off and assessed in xylose media. It was found that these colonies inherited their ability of xylose metabolic adaptation after being grown on glucose. It was observed that the growth of CA271 derivatives from metabolic adaptation were improved by 3-fold, compared to the original unadapted CA271. To understand whether this is caused by a mutation, the XR and XDH genes were sequenced. Sequencing of the xylose genes in the CA271 derivatives showed no genetic changes, suggesting xylose metabolic adaptation may be caused by alterations elsewhere in the genome.

The second way to improve the growth on xylose was to investigate the function of the N-terminus of *C. albicans*, which has a 55 amino acid extension that is unique in its fungal species. A fusion protein was constructed that consisted of the N-terminus of *CaGRE3* with *ScGRE3*. This mutant *GRE3* was transformed into both *S. cerevisiae* and *C. albicans* and assessed for growth. It was observed that when the chimeric Gre3p was transformed into *gre3* and CA270, there was significant improvement compared to their predecessors CA256 and CA271. There was a 4-fold increase in growth between AL002 and CA256, and a 23-fold increase in growth between AL003 and CA271. To ensure this was due to the chimeric *GRE3*, primers were designed for the *RPS1* integration site as well as for the chimeric *GRE3* for PCR confirmation. pAL001, pAL002 and pAL003 were re-streaked to assess plasmid stability (data not shown). This supports the idea that the N-terminus of *Ca*GRE3p contributes some advantage in the coupling between the XR and XDH. Based on examination of the crystal structure of *C. tenuis* GRE3p using JMol, it was observed that the N-terminus is on the opposite side of the active site, suggesting that it is less likely that the enzymatic function of *ScGRE3* has been improved

(Kavanagh, Klimacek, Nidetzky, & Wilson, 2002). The addition of the *CaGRE3* terminus protrudes away from the TIM barrel active site, suggesting that the chimeric GRE3p could be coupling better with *Sc*SOR1p. This hypothesis could be tested by examining the interaction between the chimeric GRE3p and SOR1p in *S. cerevisiae*. Other possibilities how the N-terminus of *CaGRE3* is enhancing xylose metabolism could be that it is increasing the stability of *ScGRE3*, guiding the protein to a different localization, or creating an allosteric enzymatic function.

To understand xylose catabolism even further, metabolite analysis was performed on wild type, CA271 and the CA271 adapted strains. It was observed that wild type had relatively lower concentrations of xylose, and compared to CA271 and adapted strains. This supports the idea that *CaGRE3* metabolizes xylose better in *Candida*, than *ScGRE3*. There were relatively higher concentrations of xylitol in the wild type, suggesting that xylose is being metabolized to xylitol more efficiently. The same trend was observed for xylulose, in that there were relatively higher concentrations in the wild type, compared to CA271 and the adapted strains. It was also observed that the adapted strains had slightly higher amounts of the three metabolites. This suggests that the adapted could be more efficient in importing xylose, and metabolizing xylose and xylitol. It is still unknown on what made the adapted strains more efficient in a xylose environment compared to the original CA271 strain.

It was found that *C. albicans* could use amino acids as a carbon source. To investigate this, wild type and *gre3/xyl2* were subjected to glucogenic and ketogenic amino acids as the sole carbon source. Growth was observed on glucogenic but not ketogenic amino acids. This correlates with humans because glucogenic amino acids are

glucose precursors, whereas ketogenic amino acids are precursors for fatty acids and ketone bodies. This was taken one step further by growing wild type and *gre3/xyl2* in single glucogenic amino acids. It was found that out of the thirteen amino acids, growth was observed on seven of the glucogenic amino acids (serine, proline, alanine, glutamate, glutamine, aspartate, asparagine). It was observed that key enzymes in the other four glucogenic amino acids in humans were not present in *C. albicans*. The enzymes to convert glycine and arginine into gluconeogenic precursors are present in *C. albicans*, although the strains did not grow. It was speculated why *gre3/xyl2* was not growing in xylose medium, although it had the necessary amino acids to convert into gluconeogenic precursors. In humans, it has been shown that amino acid metabolism is decreased by a high carbohydrate diet, and it is increased during prolonged starvation (Felig, Owen, Wahren, & Cahill, 1969). This suggests that there is some regulation mechanism between detecting a carbohydrate environment and a low to no carbohydrate environment. It is interesting that despite the *gre3/xyl2* not having the enzymes for xylose metabolism, the transported xylose in the cell and in the extracellular environment gives a signal to inhibit amino acid catabolism. Similar to *S. cerevisiae*, *C. albicans* possesses an amino acid sensing mechanism called the SPS-sensor pathway, which senses and responds to extracellular amino acids, which extracellular amino acids induce the proteolytic processing of *Candida STP1* and *STP2* homologs, which activates multiple systems for amino acid uptake (Martínez & Ljungdahl, 2005). It was found that *Candida* cells lacking the ability to respond and take up amino acids were unable to establish virulent infections in mouse model (Martínez & Ljungdahl, 2004). This correlates with the idea that amino acid catabolism is necessary for *Candida* to survive in its sugar-limiting niches. It was

suggested that sugars have some connection with the amino acid sensors in which, are associated with the amino acid permeases. If we knew what that connection was, it would help understood why *Candida gre3/xyl2* is not using the glucogenic amino acids in the xylose medium to survive.

Comparative genomics studies have showed that the XR and XDH genes of *S. cerevisiae* and *C. albicans* are well conserved. So why is it that *C. albicans* can grow on xylose and *S. cerevisiae* cannot? Understanding carbon metabolism in *C. albicans* can perhaps not only understand the way *Candida* behaves during an infection, but help us understand xylose metabolism in *S. cerevisiae*, which could potentially lead to understanding how to utilize xylose for ethanol fermentation.

References

Barelle, C. J., Priest, C. L., Maccallum, D. M., Gow, N. A. R., Odds, F. C., & Brown, A. J. P. (2006). Niche-specific regulation of central metabolic pathways in a fungal pathogen. *Cellular microbiology*, *8*(6), 961–971. doi:10.1111/j.1462-5822.2005.00676.x

Beck-Sagué, C., & Jarvis, W. R. (1993). Secular trends in the epidemiology of nosocomial fungal infections in the United States, 1980-1990. National Nosocomial Infections Surveillance System. *The Journal of infectious diseases*, *167*(5), 1247–1251.

Bezerra, A. R., Simões, J., Lee, W., Rung, J., Weil, T., Gut, I. G., Gut, M., et al. (2013). Reversion of a fungal genetic code alteration links proteome instability with genomic and phenotypic diversification. *Proceedings of the National Academy of Sciences of the United States of America*, *110*(27), 11079–11084. doi:10.1073/pnas.1302094110

Brat, D., Boles, E., & Wiedemann, B. (2009). Functional expression of a bacterial xylose isomerase in Saccharomyces cerevisiae. *Applied and environmental microbiology*, *75*(8), 2304–2311. doi:10.1128/AEM.02522-08

Brown, A. J. P., Brown, G. D., Netea, M. G., & Gow, N. A. R. (2014a). Metabolism impacts upon Candida immunogenicity and pathogenicity at multiple levels. *Trends in microbiology*, *22*(11), 614–622. doi:10.1016/j.tim.2014.07.001

Brown, A. J. P., Budge, S., Kaloriti, D., Tillmann, A., Jacobsen, M. D., Yin, Z., Ene, I. V., et al. (2014b). Stress adaptation in a pathogenic fungus. *The Journal of experimental biology*, *217*(Pt 1), 144–155. doi:10.1242/jeb.088930

Carlson, M. (1999). Glucose repression in yeast. *Current opinion in microbiology*, *2*(2), 202–207. doi:10.1016/S1369-5274(99)80035-6

Deng, X. X., & Ho, N. W. (1990). Xylulokinase activity in various yeasts including Saccharomyces cerevisiae containing the cloned xylulokinase gene. Scientific note. *Applied biochemistry and biotechnology*, *24-25*, 193–199.

Felig, P., Owen, O. E., Wahren, J., & Cahill, G. F. (1969). Amino acid metabolism during prolonged starvation. *The Journal of clinical investigation*, *48*(3), 584–594. doi:10.1172/JCI106017

Goddard, M. R., & Greig, D. (2015). Saccharomyces cerevisiae: a nomadic yeast with no niche? *FEMS yeast research*, *15*(3). doi:10.1093/femsyr/fov009

Hahn-Hägerdal, B., Karhumaa, K., Jeppsson, M., & Gorwa-Grauslund, M. F. (2007). Metabolic engineering for pentose utilization in Saccharomyces cerevisiae. *Advances in biochemical engineering/biotechnology*, *108*, 147–177. doi:10.1007/10_2007_062

Harcus, D., Dignard, D., Lépine, G., Askew, C., Raymond, M., Whiteway, M., & Wu, C. (2013). Comparative Xylose Metabolism among the Ascomycetes C. albicans, S. stipitis and S. cerevisiae. *PloS one*, *8*(11), e80733. doi:10.1371/journal.pone.0080733

Hothersall, J. S., & Ahmed, A. (2013). Metabolic fate of the increased yeast amino Acid uptake subsequent to catabolite derepression. *Journal of amino acids*, *2013*, 461901. doi:10.1155/2013/461901

Huang, G. (2012). Regulation of phenotypic transitions in the fungal pathogen Candida albicans. *Virulence*, *3*(3), 251–261. doi:10.4161/viru.20010

Kavanagh, K. L., Klimacek, M., Nidetzky, B., & Wilson, D. K. (2002). The structure of apo and holo forms of xylose reductase, a dimeric aldo-keto reductase from Candida

tenuis. *Biochemistry*, *41*(28), 8785–8795.
Klein, R. S., Harris, C. A., Small, C. B., Moll, B., Lesser, M., & Friedland, G. H. (1984). Oral candidiasis in high-risk patients as the initial manifestation of the acquired immunodeficiency syndrome. *The New England journal of medicine*, *311*(6), 354–358. doi:10.1056/NEJM198408093110602
Lan, C.-Y., Newport, G., Murillo, L. A., Jones, T., Scherer, S., Davis, R. W., & Agabian, N. (2002). Metabolic specialization associated with phenotypic switching in Candidaalbicans. *Proceedings of the National Academy of Sciences of the United States of America*, *99*(23), 14907–14912. doi:10.1073/pnas.232566499
Lin, S.-J., Kaeberlein, M., Andalis, A. A., Sturtz, L. A., Defossez, P.-A., Culotta, V. C., Fink, G. R., et al. (2002). Calorie restriction extends Saccharomyces cerevisiae lifespan by increasing respiration. *Nature*, *418*(6895), 344–348. doi:10.1038/nature00829
Lorenz, M. C. (2013). Carbon catabolite control in Candida albicans: new wrinkles in metabolism. *mBio*, *4*(1), e00034–13. doi:10.1128/mBio.00034-13
Lorenz, M. C., Bender, J. A., & Fink, G. R. (2004). Transcriptional response of Candida albicans upon internalization by macrophages. *Eukaryotic cell*, *3*(5), 1076–1087. doi:10.1128/EC.3.5.1076-1087.2004
Madhavan, A., Tamalampudi, S., Ushida, K., Kanai, D., Katahira, S., Srivastava, A., Fukuda, H., et al. (2009). Xylose isomerase from polycentric fungus Orpinomyces: gene sequencing, cloning, and expression in Saccharomyces cerevisiae for bioconversion of xylose to ethanol. *Applied microbiology and biotechnology*, *82*(6), 1067–1078. doi:10.1007/s00253-008-1794-6
Martínez, P., & Ljungdahl, P. O. (2004). An ER packaging chaperone determines the amino acid uptake capacity and virulence of Candida albicans. *Molecular microbiology*, *51*(2), 371–384. doi:10.1046/j.1365-2958.2003.03845.x
Martínez, P., & Ljungdahl, P. O. (2005). Divergence of Stp1 and Stp2 transcription factors in Candida albicans places virulence factors required for proper nutrient acquisition under amino acid control. *Molecular and cellular biology*, *25*(21), 9435–9446. doi:10.1128/MCB.25.21.9435-9446.2005
Matsushika, A., Inoue, H., Kodaki, T., & Sawayama, S. (2009). Ethanol production from xylose in engineered Saccharomyces cerevisiae strains: current state and perspectives. *Applied microbiology and biotechnology*, *84*(1), 37–53. doi:10.1007/s00253-009-2101-x
Miller, L. G., Hajjeh, R. A., & Edwards, J. E. (2001). Estimating the cost of nosocomial candidemia in the united states. *Clinical infectious diseases : an official publication of the Infectious Diseases Society of America*, *32*(7), 1110. doi:10.1086/319613
Mosier, N., Wyman, C., Dale, B., Elander, R., Lee, Y. Y., Holtzapple, M., & Ladisch, M. (2005). Features of promising technologies for pretreatment of lignocellulosic biomass. *Bioresource technology*, *96*(6), 673–686. doi:10.1016/j.biortech.2004.06.025
Nantel, A., Rigby, T., & Hogues, H. (2006). Microarrays for studying pathogenicity in Candida albicans. *... mycology: cellular and ...*.
Peter, G. J., Düring, L., & Ahmed, A. (2006). Carbon catabolite repression regulates amino acid permeases in Saccharomyces cerevisiae via the TOR signaling pathway. *The Journal of biological chemistry*, *281*(9), 5546–5552.

doi:10.1074/jbc.M513842200
Ryan, D., & Robards, K. (2006). Metabolomics: The greatest omics of them all? *Analytical chemistry*, *78*(23), 7954–7958. doi:10.1021/ac0614341
Saloheimo, A., Rauta, J., Stasyk, O. V., Sibirny, A. A., Penttilä, M., & Ruohonen, L. (2007). Xylose transport studies with xylose-utilizing Saccharomyces cerevisiae strains expressing heterologous and homologous permeases. *Applied microbiology and biotechnology*, *74*(5), 1041–1052. doi:10.1007/s00253-006-0747-1
Slininger, P. J., Bothast, R. J., Van Cauwenberge, J. E., & Kurtzman, C. P. (1982). Conversion of D-xylose to ethanol by the yeast Pachysolen tannophilus. *Biotechnology and bioengineering*, *24*(2), 371–384. doi:10.1002/bit.260240210
Somerville, C. (2007). Biofuels. *Current biology : CB*, *17*(4), R115–9. doi:10.1016/j.cub.2007.01.010
Sudbery, P., Gow, N., & Berman, J. (2004). The distinct morphogenic states of Candida albicans. *Trends in microbiology*, *12*(7), 317–324. doi:10.1016/j.tim.2004.05.008
van der Werf, M. J., Jellema, R. H., & Hankemeier, T. (2005). Microbial metabolomics: replacing trial-and-error by the unbiased selection and ranking of targets. *Journal of industrial microbiology & biotechnology*, *32*(6), 234–252. doi:10.1007/s10295-005-0231-4
Young, E. M., Tong, A., Bui, H., Spofford, C., & Alper, H. S. (2014). Rewiring yeast sugar transporter preference through modifying a conserved protein motif. *Proceedings of the National Academy of Sciences of the United States of America*, *111*(1), 131–136. doi:10.1073/pnas.1311970111
Young, E., Lee, S.-M., & Alper, H. (2010). Optimizing pentose utilization in yeast: the need for novel tools and approaches. *Biotechnology for biofuels*, *3*, 24. doi:10.1186/1754-6834-3-24
Young, E., Poucher, A., Comer, A., Bailey, A., & Alper, H. (2011). Functional survey for heterologous sugar transport proteins, using Saccharomyces cerevisiae as a host. *Applied and environmental microbiology*, *77*(10), 3311–3319. doi:10.1128/AEM.02651-10

Figure Legends

Figure 1. Xylose entry to the pentose phosphate pathway. The schematic presentation of conserved genes encoding enzymatic activities for xylose entry into the PPP pathway in *S. cerevisiae* and *C. albicans*.

Figure 2. Metabolizing capacities of *C. albicans* mutants and rescued strains. (A) Growth of *C. albicans* strains in SC with 2% xylose. Strains SC5314, *gre3, xyl2, gre3/xyl2,* CA256, CDH139 and CA271 were grown aerobically at 30^{o}C and the growth was measured over a period of 12 days in 96-well plates. **(B)** The xylose reductase and xylitol dehydrogenase genes from *S. cerevisiae* complement *C. albicans* deletion mutants of the corresponding genes. The *C. albicans* wild type SC5314 was used as a positive control; *S. cerevisiae* wild type BY4743 and *C. albicans gre3*, *xyl2* and *gre3/xyl2* were used as negative controls. *S. cerevisiae GRE3* (CA256), *S. cerevisiae SOR1* (CDH139) and *S. cerevisiae GRE3*/*SOR1* complement the *C. albicans gre3*, *xyl2* and *gre3/xyl2* mutants, respectively. Strains were grown aerobically at 30^{o}C in 2% xylose. The optical density was measured over a period of 30 days, n =5. **(C)** *S. cerevisiae, gre3, xyl2* and *gre3/xyl2* were used as negative controls (first row). The *C. albicans* wild type SC5314, CA256 (*gre3::ScGRE3*), CDH139 (*xyl2::ScSOR1*) and CA271 (*gre3/xyl2::ScGRE3/SOR1*) were used as positive controls (second row). *gre3* and CA270 were complemented with *CaScGRE3* to create AL002 and AL003 (third row). Strains were grown aerobically at 30^{o}C in 2% xylose solid plates. Scans were taken daily. **(D)** Strains were grown aerobically at 30^{o}C and the growth (OD) was measured over a period of 5 days in 96-well plates, n =12. Growth was quantified using the TECAN plate

reader. All of the axes (x and y) are on the same scale. Rows: SC5314 (A), BY4743 (B), CA256 (C), CDH139 (D), CA271 (E), AL002 (F), AL003 (G). **(E)** *S. cerevisiae, gre3, xyl2* and *gre3/xyl2* were used as negative controls (first row). The *C. albicans* wild type SC5314, CA256 (*gre3::ScGRE3*), CDH139 (*xyl2::ScSOR1*) and CA271 (*gre3/xyl2::ScGRE3/SOR1*) were used as positive controls (second row). *gre3* and CA270 were complemented with *CaScGRE3* to create AL002 and AL003 (third row). Strains were grown aerobically at 30^{o}C in 2% xylose solid plate. Scans were taken daily.

Figure 3. Alignment of the xylose reductase *GRE3* in the fungal kingdom. The alignment was performed using the program MAFFT. There is a ~55 amino acid N-terminal extension that is present in *C. albicans* that is missing in *S. cerevisiae*. *C. albicans* seems to have to most "extended" N-terminus relative to the other fungal species.

Figure 4. Transcription profile of *C. albicans* wild type, *gre3/xyl2* and CA271 in xylose. Microarray experiments with *C. albicans* grown in xylose. **(A)** Upregulated genes of wild type when compared to *gre3/xyl2*. **(B)** Upregulated genes of CA271 when compared to *gre3/xyl2*. **(C)** Upregulated genes of wild type when compared to CA271.

Figure 5. *gre3/xyl2* and CA271 grown on xylose agarose plates for six days then grown in xylose media for three days. (A) The strains were streaked on plates with no dilution (on the left), and with 1:100 dilution (on the right). **(B)** The first three rows depict *gre3/xyl2* from the xylose plate and the last five rows depict CA271. It was

observed that only the CA271 colonies from the xylose plate were able to grow in xylose media. **(C)** Growth of adapted CA271 mutants compared to the wild type and unadapted CA271. Strains were grown aerobically at 30^{o}C in 2% xylose. The optical density was measured over a period of 30 days, n = 3.

Figure 6. Creation, integration and confirmation of *CaScGRE3* construct. (A) Plasmid pl396 was digested with *Kpn*I/*Spe*I to give rise to two bands: 4319bp (CIpACT1-CYC backbone) and 2993bp (*ScGRE3*)(Lane 2). CIpACT1-CYC was also digested with *Kpn*I/*Spe*I to compare the backbone with pl396 (Lane 3). pRS314 was digested with *Kpn*I/*Spe*I (Lane 4). pRS314 and *ScGRE3* were ligated to create pAL001. pAL001 was digested wit *Kpn*I/*Spe*I to yield the pRS314 backbone as well as *ScGRE3* (Lane 6). The N-terminus of *CaGRE3* was amplified by PCR to give a band of 455bp (Lane 7). pAL001 and the N-terminus fragment were recombined to give rise to pAL002. pAL002 was digested with *Kpn*I/*Spe*I to give rise to two bands (Lane 9). *CaScGRE3* was re-ligated into CIpACT1-CYC to give rise to pAL003 (Lane 10). pAL003 digested with *Kpn*I/*Spe*I created two bands (Lane 11). **(B)** Confirmation of *CaScGRE3 construct*. pAL003 was amplified with primers OAL003 and OAL004 to confirm the homologous recombination of the *CaScGRE3* gene. PCR product was sent for Sanger sequencing at Genome Quebec, Submission #165761, June 18th, 2014. **(C)** Different possibilities of integration of CaScGRE3 at the ACT1p and RPS1 locus. To re-create the double complemented strain, CA270 was complemented with *CaScGRE3* to give rise to AL003. Since *ScSOR1* was already present in one of the locus, *CaScGRE3* had a 50% chance of integrating in the correct diploid locus. **(D)** Confirmation of successful and unsuccessful AL003

transformants. PCR was performed between the ACT1p and *RPS1* locus from isolated gDNA of various transformants. Successful AL003 transformants two bands, which consisted of *CaScGRE3* and *ScSOR1*. Unsuccessful transformants showed the slight presence of *CaScGRE3* but not *ScSOR1* (see Figure 6C for placement of oligonucleotides). **(E)** The xylose reductase and xylitol dehydrogenase genes from *S. cerevisiae* complement *C. albicans* deletion mutants of the corresponding genes. AL002 and AL003 were complemented with the engineered *CaScGRE3*. CA256 was compared to AL002 and CA271 to AL003. Strains were grown aerobically at 30^{o}C in 2% xylose. The optical density was measured over a period of 30 days, n =3.

Figure 7. Metabolite analysis of intracellular xylose, xylitol and xylulose during mid-log phase of growth. (A) The relative ratio (compared to WT) of xylose was measured between CA271 and four adapted strains. CA271 had ≈5 times more xylose than the WT. The adapted strains had relatively slightly more xylose than CA271. **(B)** The relative ratio (compared to WT) of xylitol and xylulose was measured between CA271 and four adapted strains. CA271 had ≈5 times less of the two metabolites compared to the WT. The adapted strains had relatively slightly more xylitol and xylulose compared to CA271.

Figure 8. Assessment of WT, *gre3*, *xyl2*, *gre3/xyl2*, CA256, CDH139 and CA271 on xylose and amino acids. (A) Mutants for *gre3* and/or *xyl2* were not able to grow on xylose. However, when these strains grow on amino acids as the sole carbon, growth was observed over a period of 2-3 days. Serial dilutions were created for each strain, from left to right. **(B)** Growth of WT and *gre3/xyl2* was observed over a period of eight hours on

either glucogenic or ketogenic amino acids. Both medias were supplemented with adenine and uridine for *Candida albicans*. **(C)** WT and *gre3/xyl2* were grown on 13 single glucogenic amino acids from *H. sapiens*. Out of the 13, growth was observed on seven of the glucogenic amino acids. The OD for WT and *gre3/xyl2* were very similar and compiled into one curve. Growth was measured over 7 days.

Figure S1. Growth of *C. albicans* on glucogenic amino acids. Thirteen glucogenic amino were chosen based on humans. *C. albicans* WT and *gre3/xyl2* were grown on these amino acids as the only source of carbon. It was observed that the pathogen lacks some of the necessary enzymes to metabolize Cys, His, Met and Val, and does not grow. The pathogen has the enzymes to metabolism Arg and Gly but is still unable to grow. Presence and absence of enzymes was verified through the Candida Genome Database.

Figure S2. Plasmid map of pAL001. This plasmid contains *ScGRE3* in the pRS314 vector backbone. Plasmid map was generated using the program MacVector.

Figure S3. Plasmid map of pAL002. This plasmid contains *CaScGRE3* in the pRS314 vector backbone. Plasmid map was generated using the program MacVector.

Figure S4. Plasmid map of pAL003. This plasmid contains *CaScGRE3* in the CIpACT1-CYC vector backbone. Plasmid map was generated using the program MacVector.

Figure S5. Adapted-evolution growth assay conditions. The double complemented strain CA271 was plated in three different conditions before assayed in liquid xylose: (A) Plated on 2% glucose. (B) Plated on 2% xylose. (C) Plated on 2% xylose, then replica plated on 2% glucose.

Figure S6. Adapted-evolution growth assay on Day 5. CA271 colonies plated in condition (B) or (C) showed improved growth compared to (A).

Figure 1

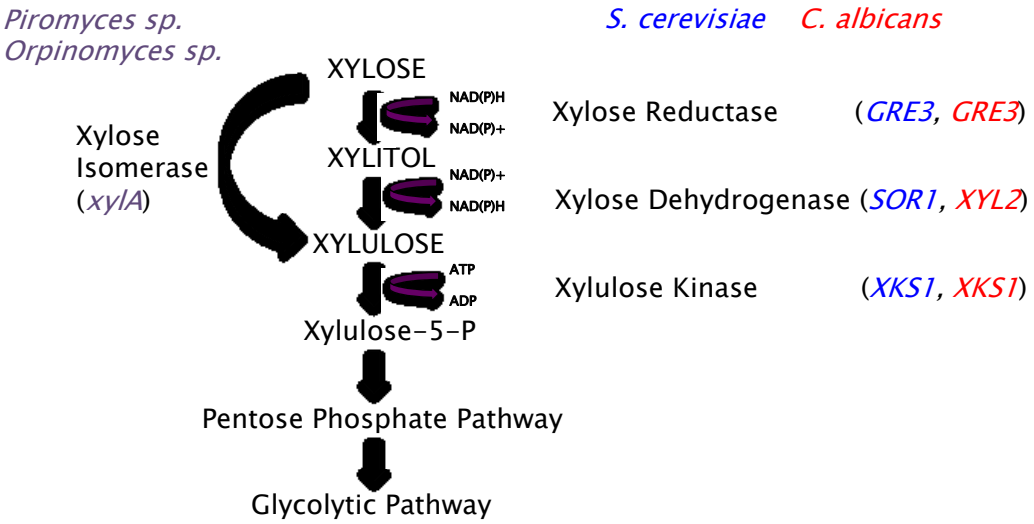
Piromyces sp.
Orpinomyces sp.
S. cerevisiae
C. albicans
XYLOSE
NAD(P)H
NAD(P)+
XYLITOL
NAD(P)+
NAD(P)H
XYLULOSE
ATP
ADP
Xylulose-5-P
Pentose Phosphate Pathway
Glycolytic Pathway
Xylose Isomerase (xylA)
Xylose Reductase (GRE3, GRE3)
Xylose Dehydrogenase (SOR1, XYL2)
Xylulose Kinase (XKS1, XKS1)

Figure 2A

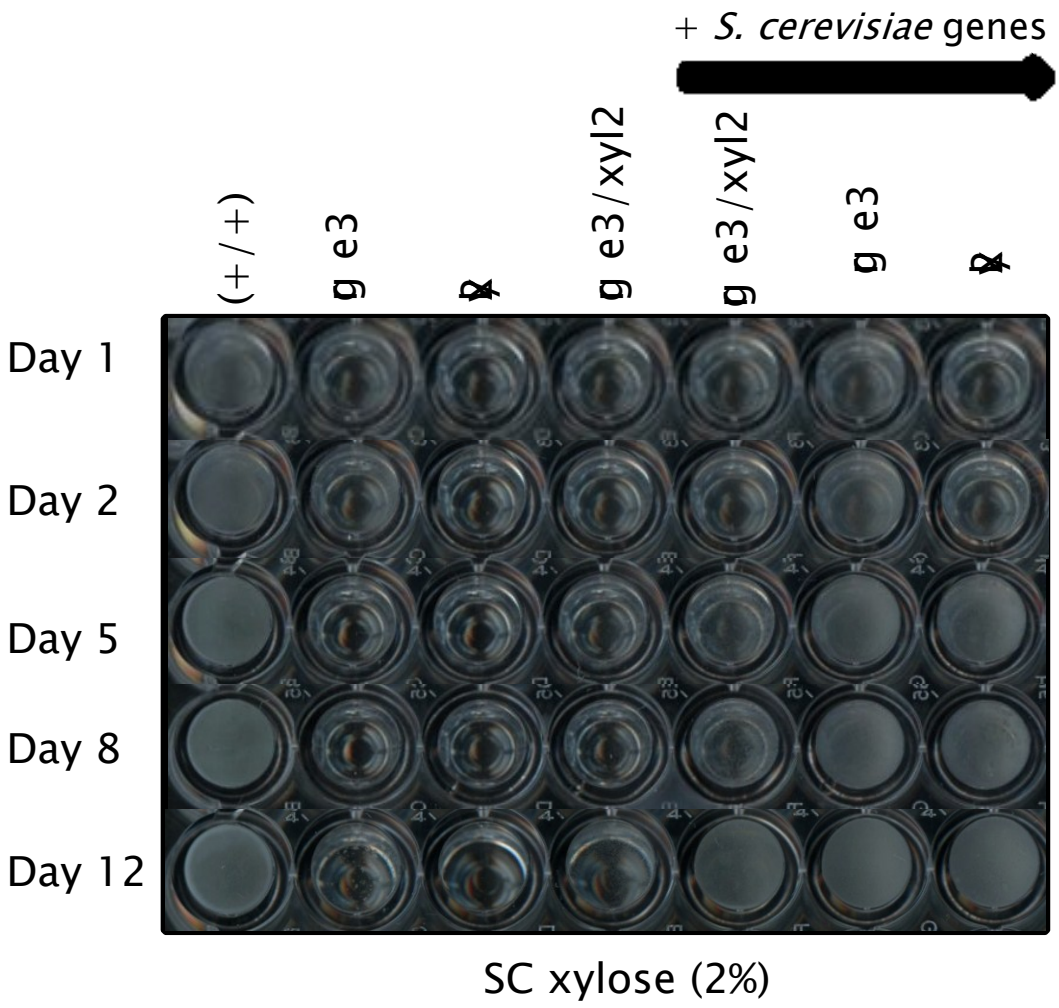
+ S. cerevisiae genes
(+/+)
g e3
g e3/xyl2
g e3/xyl2
g e3
Day 1
Day 2
Day 5
Day 8
Day 12
SC xylose (2%)

Figure 2B

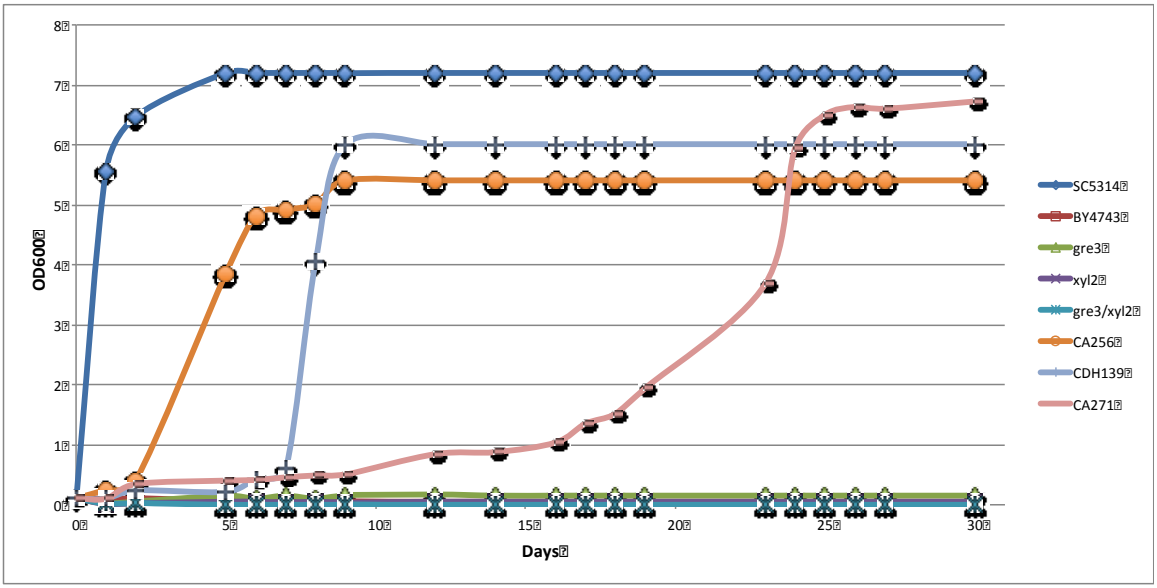
OD600
Days
0
5
10
15
20
25
30
SC5314
BY4743
gre3
xyl2
gre3/xyl2
CA256
CDH139
CA271

Figure 2C

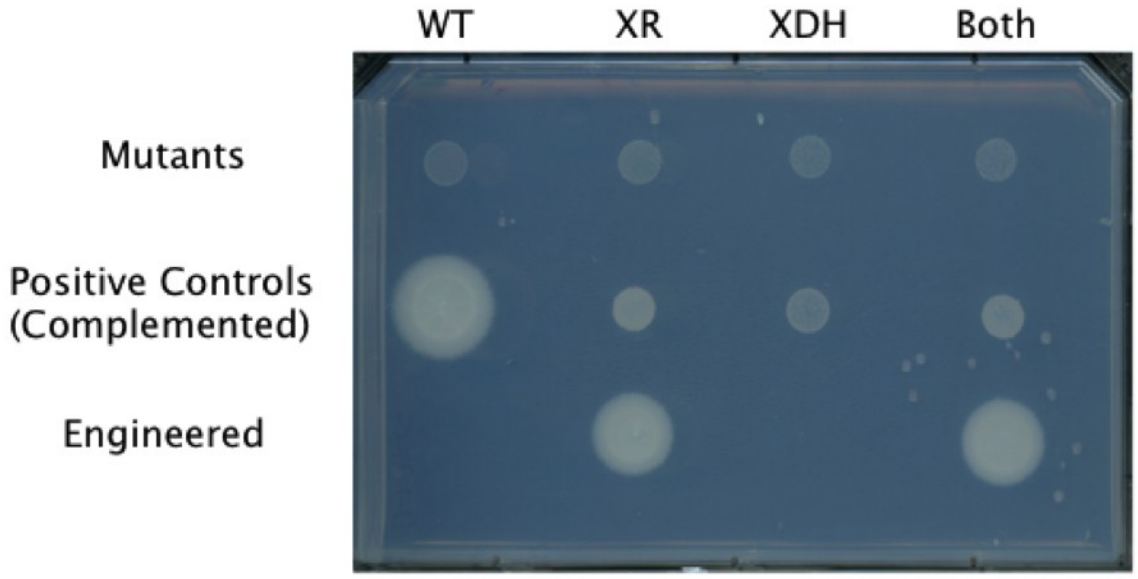
WT
XR
XDH
Both
Mutants
Positive Controls
(Complemented)
Engineered

Figure 2D

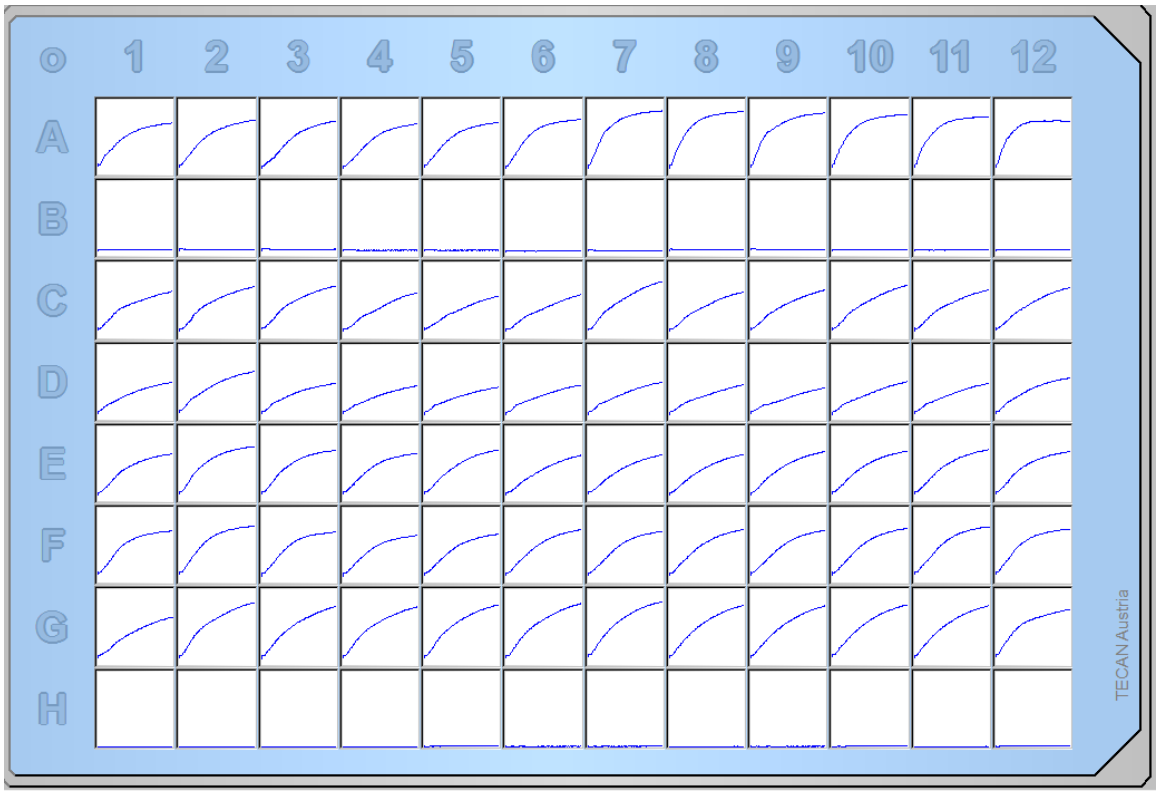

Figure 2E

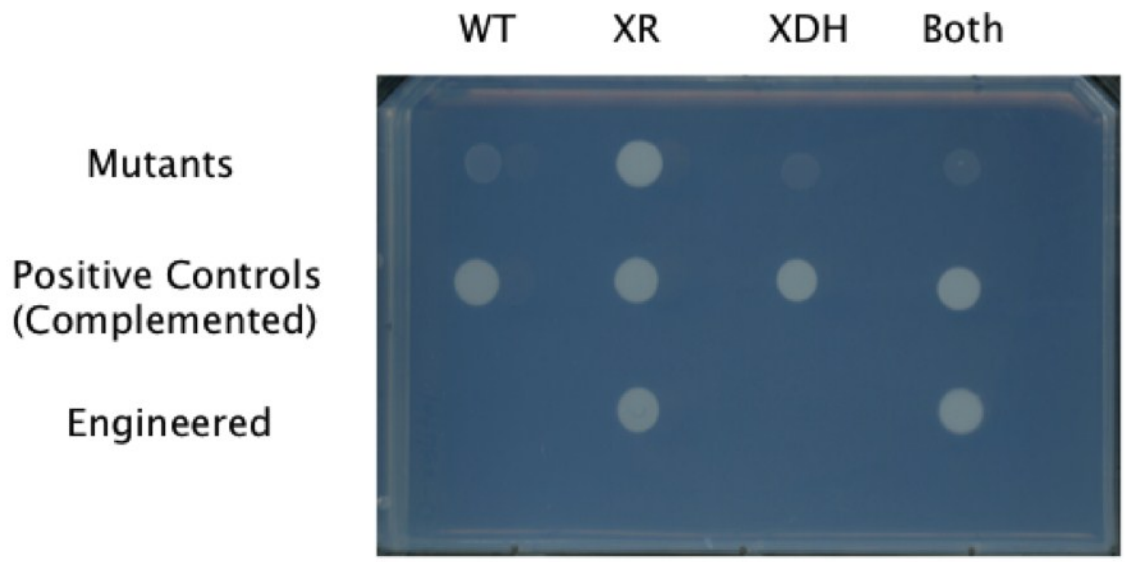
WT
XR
XDH
Both
Mutants
Positive Controls
(Complemented)
Engineered

Figure 3

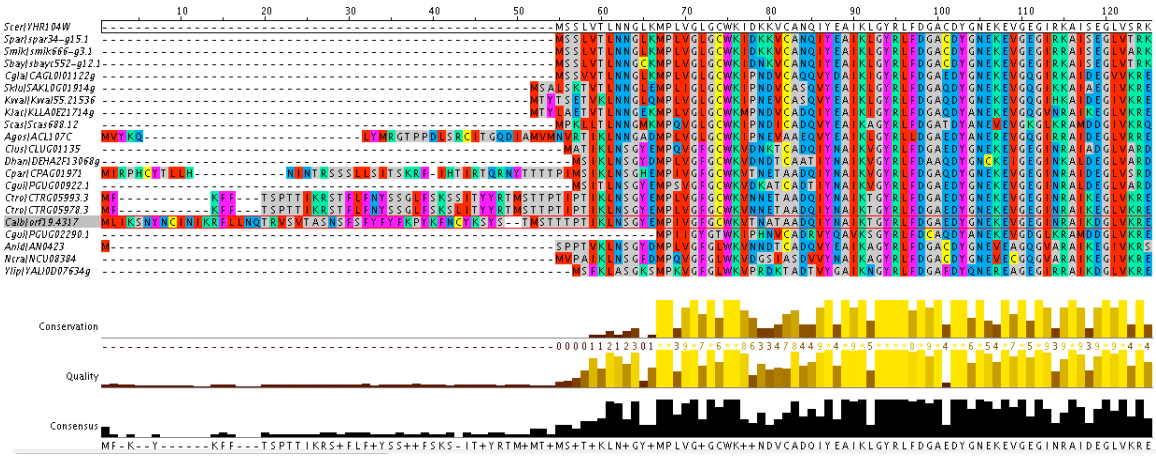

Figure 4A

CGD orf	WT vs. null in SX	CGD Name	Process
orf19.4317	301.9175	GRE3	D-xylose catabolic process
orf19.7585	248.171	INO1	carb metabolic process
orf19.7676	137.805	XYL2	redox process
orf19.1715	24.922	IRO1	iron ion homeostasis
orf19.5971	18.523	MTC6 ortholog	-
orf19.6486	18.4055	LDG3	-
orf19.1982	12.4795	-	aerobic respiration
orf19.5437	12.2255	RHR2	cell-abiotic subtrate adhesion
orf19.4402	10.87	-	-
orf19.5587	7.4925	-	cellular response to methylmercury
orf19.1587	7.2455	-	carbohydrate transport
orf19.4444	7.122	-	phenotype switching
orf19.4773	6.672	AOX2	alternative respiration
orf19.1614	6.6245	MEP1	ammonium transport
orf19.2108	6.4985	SOD6	redox process
orf19.5025	6.3245	MET3	sulfate assimilation
orf19.11	5.468	-	-
orf19.339	5.1835	NDE1	NADH oxidation
orf19.38	4.8775	-	-
orf19.6814	4.7935	TDH3	redox process
orf19.1868	4.761	RNR22	redox process
orf19.7680	4.705	CTA26	positive reg of transcription
orf19.2532	4.5995	PRS	prolyl-tRNA aminoacylation
orf19.5305	4.48	RHD3	fungal-type cell wall organization
orf19.3575	4.375	CDC19	cellular response to starvation
orf19.395	4.276	ENO1	carbon utilization
orf19.5620	4.2395	-	biocsynthetic process
orf19.6959	4.0665	HOM32	-
orf19.1306	4.0135	-	redox process

Expression Level: No Data | <0.5 | 0.5–2 | >2–6 | >6–10 | >10

Figure 4B

CGD orf	CA271 vs. null in SX	CGD Name	Process
orf19.4317	105.2631579	GRE3	D-xylose catabolic process
orf19.6486	23.52941176	LDG3	-
orf19.7585	15.50387597	INO1	inositol biosynthetic process
orf19.616	14.18439716	-	-
orf19.1715	11.9047619	IRO1	cellular iron ion homeostasis
orf19.1614	11.83431953	MEP1	ammonium transport
orf19.4444	10.47120419	PHO15	phenotypic switching
orf19.2645	8.695652174	-	-
orf19.1268	8.230452675	-	-
orf19.4996	8.097165992	-	-
orf19.4750	8.064516129	-	-
orf19.3121	8	GST1	-
orf19.1780	7.90513834	-	-
orf19.762	7.874015748	-	-
orf19.2445	7.843137255	-	amino acid transmembrane transport
orf19.140	7.722007722	-	-
orf19.2889	7.662835249	-	chromatin remodeling
orf19.6777	7.633587786	-	-
orf19.2681	7.547169811	RBT7	ribonuclease activity
orf19.6807	7.142857143	-	DNA integration
orf19.1763	6.666666667	IFR1	oxidation-reduction process
orf19.6366	6.666666667	-	-
orf19.4472	6.369426752	-	-
orf19.2197	6.211180124	-	oxidation-reduction process
orf19.2280	6.211180124	ZCF10	filamentous growth in response to biotic stimulus
orf19.1473	6.042296073	-	oxidation-reduction process
orf19.4239	6.024096386	-	-
orf19.57	5.917159763	PSF2	DNA-dependent DNA replication
orf19.1716	5.899705015	URA3	adhesion of symbiont to host
orf19.7665	5.763688761	-	mitochondrial respiratory chain complex IV assembly
orf19.3925	5.714285714	-	-
orf19.584	5.681818182	-	response to oxidative stress
orf19.848	5.649717514	PGA16	-
orf19.1638	5.555555556	-	ER to Golgi vesicle-mediated transport
orf19.2475	5.524861878	PGA26	cellular response to starvation
orf19.1065	5.509641873	SSA2	interaction with host
orf19.6595	5.434782609	RTA4	cellular response to starvation

Expression Level: 

Figure 4C

CGD orf	WT vs. CA271 in SX	CGD Name	Process
orf19.7676	95.23809524	XYL2	redox process
orf19.1982	16.2601626	-	role in aerobic respiration
orf19.7585	16.12903226	INO1	inositol biosynthetic process
orf19.5971	15.26717557	MTC6 ortholog	-
orf19.4402	8.888888889	-	-
orf19.4335	7.633587786	TNA1	-
orf19.5674	6.269592476	CGA10	ion homeostasis
orf19.7370	4.524886878	-	basic amino acid transmembrane export from vacuole
orf19.2532	4.237288136	PRS	prolyl-tRNA aminoacylation
orf19.2372	3.766478343	-	DNA integration
orf19.2079	3.724394786	PHHB	cellular response to starvation
orf19.4773	3.676470588	AOX2	alternative respiration
orf19.5373	3.597122302	-	-
orf19.1366	3.521126761	-	oxidation-reduction process
orf19.91	3.372681282	-	-
orf19.7278	3.294892916	-	-
orf19.1073	3.262642741	-	-
orf19.2881	3.246753247	MNN4	cell wall mannoprotein biosynthetic process
orf19.5004	3.215434084	RAD54	mitotic nuclear division
orf19.4506	3.2	LYS22	lysine biosynthetic process via aminoadipic acid
orf19.7586	3.159557662	CHT3	carbohydrate metabolic process
orf19.5556	3.086419753	-	-
orf19.1415	2.989536622	FRE10	iron ion transport
orf19.6070	2.928257687	ENA1	hyphal growth
orf19.6994	2.906976744	BAT22	branched-chain amino acid metabolic process
orf19.3526	2.820874471	ITR1	carbohydrate transport
orf19.7227	2.805049088	-	mitotic spindle assembly checkpoint
orf19.3035	2.801120448	-	mitotic sister chromatid segregation
orf19.1363	2.762430939	-	ascospore formation
orf19.468	2.75862069	-	-
orf19.6184	2.72851296	-	-
orf19.2888	2.721088435	-	ER to Golgi vesicle-mediated transport
orf19.2371	2.688172043	-	-
orf19.6950	2.649006623	-	basic amino acid transmembrane export from vacuole
orf19.822	2.649006623	HSP21	cellular response to oxidative stress
orf19.4502	2.642007926	-	rRNA processing

Expression Level: 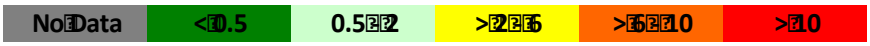

Figure 5A

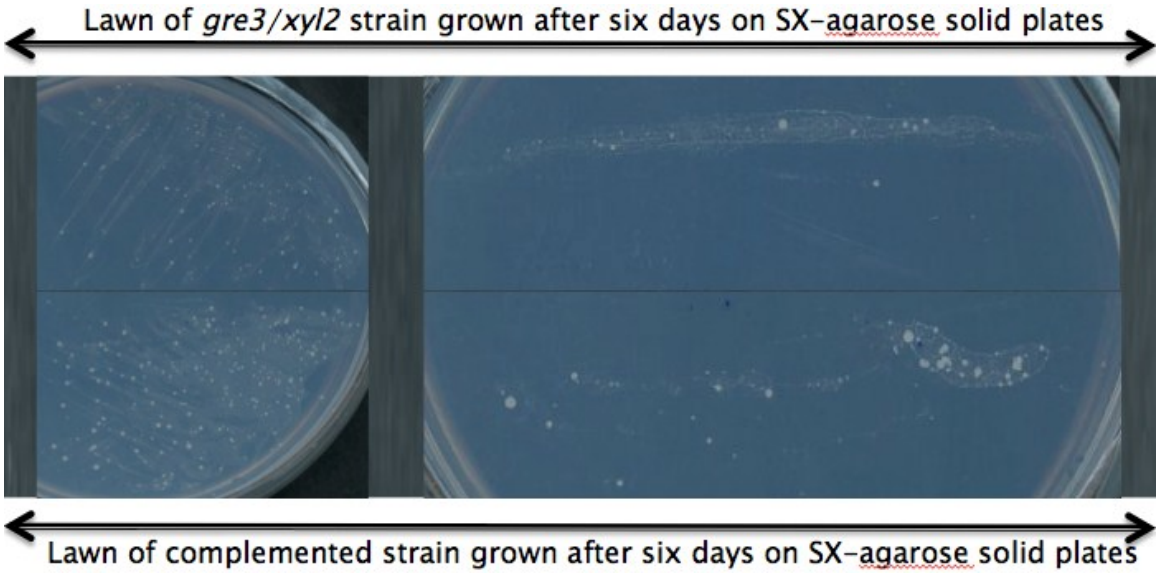
Lawn of *gre3/xyl2* strain grown after six days on SX-agarose solid plates
Lawn of complemented strain grown after six days on SX-agarose solid plates

Figure 5B

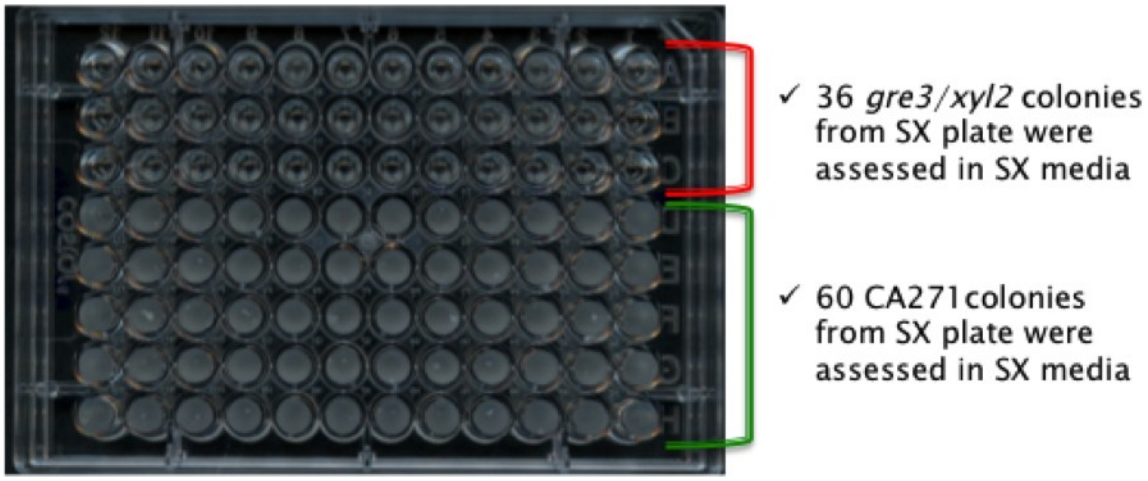
✓ 36 *gre3/xyl2* colonies from SX plate were assessed in SX media
✓ 60 CA271colonies from SX plate were assessed in SX media

Figure 5C

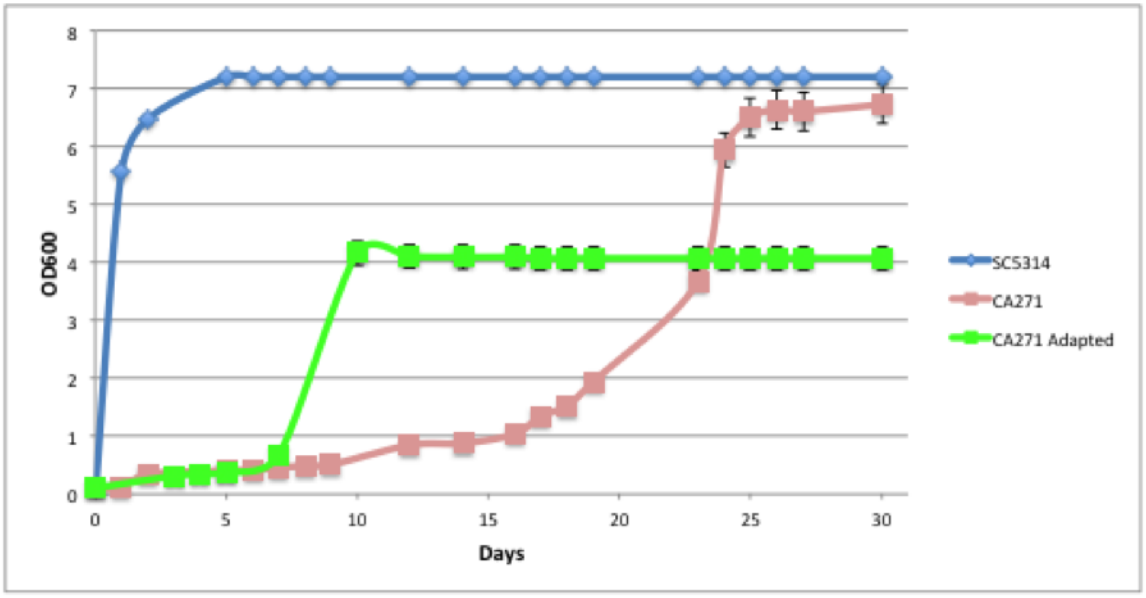
OD600
Days
0
1
2
3
4
5
6
7
8
0
5
10
15
20
25
30
SC5314
CA271
CA271 Adapted

Figure 6A

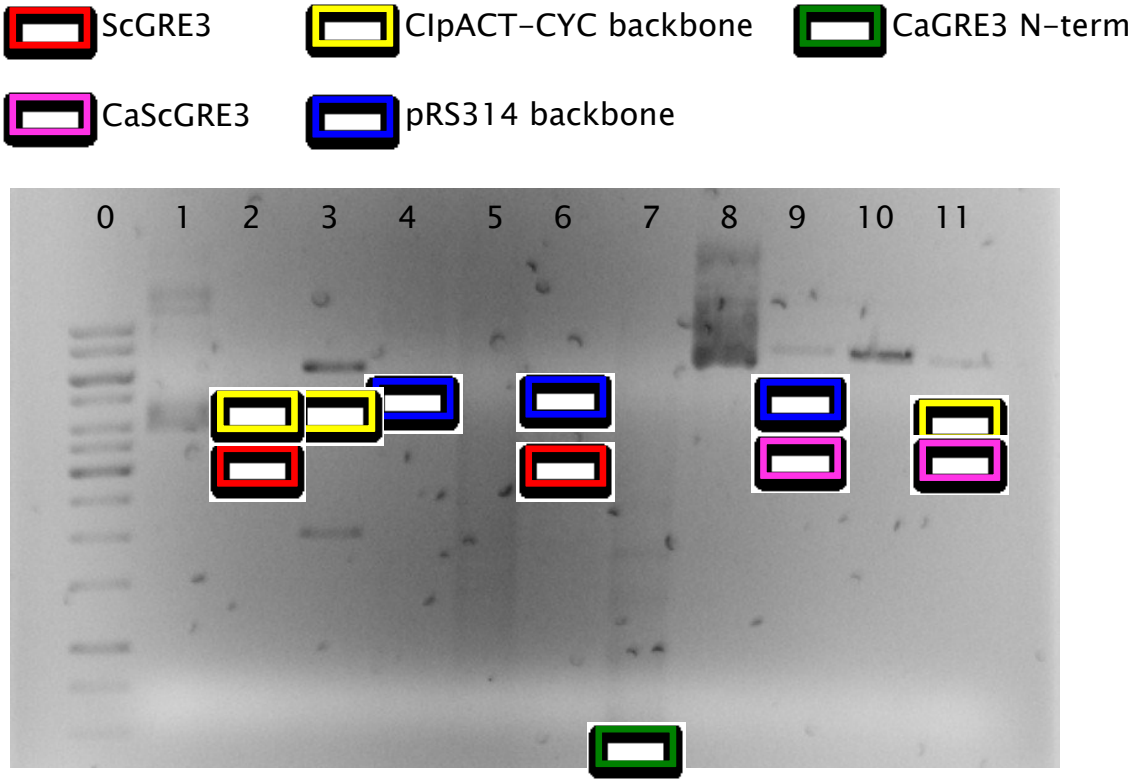
ScGRE3
ClpACT-CYC backbone
CaGRE3 N-term
CaScGRE3
pRS314 backbone
0 1 2 3 4 5 6 7 8 9 10 11

Figure 6B

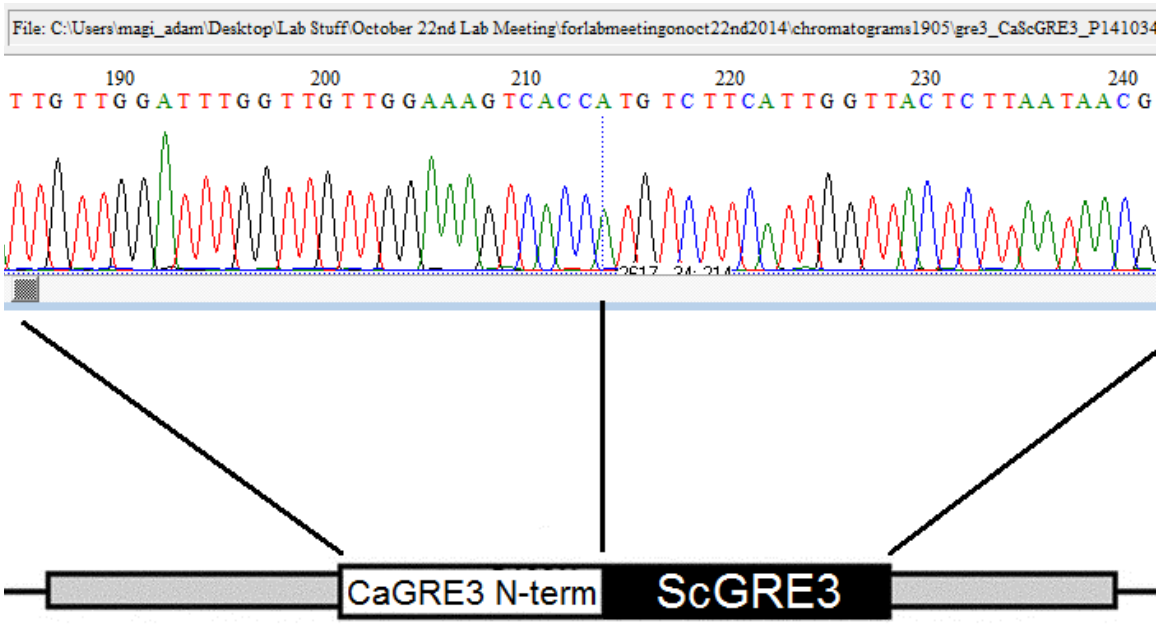
File: C:\Users\magi_adam\Desktop\Lab Stuff\October 22nd Lab Meeting\forlabmeetingonoct22nd2014\chromatograms1905\gre3_CaScGRE3_P141034
190
200
210
220
230
240
T TG T TG G AT TT GG T TG T TG G AAAG TCAC CA TG TC TTCAT TG G TTAC TC TTAATAAC G
CaGRE3 N-term
ScGRE3

Figure 6C

Scenario 1:

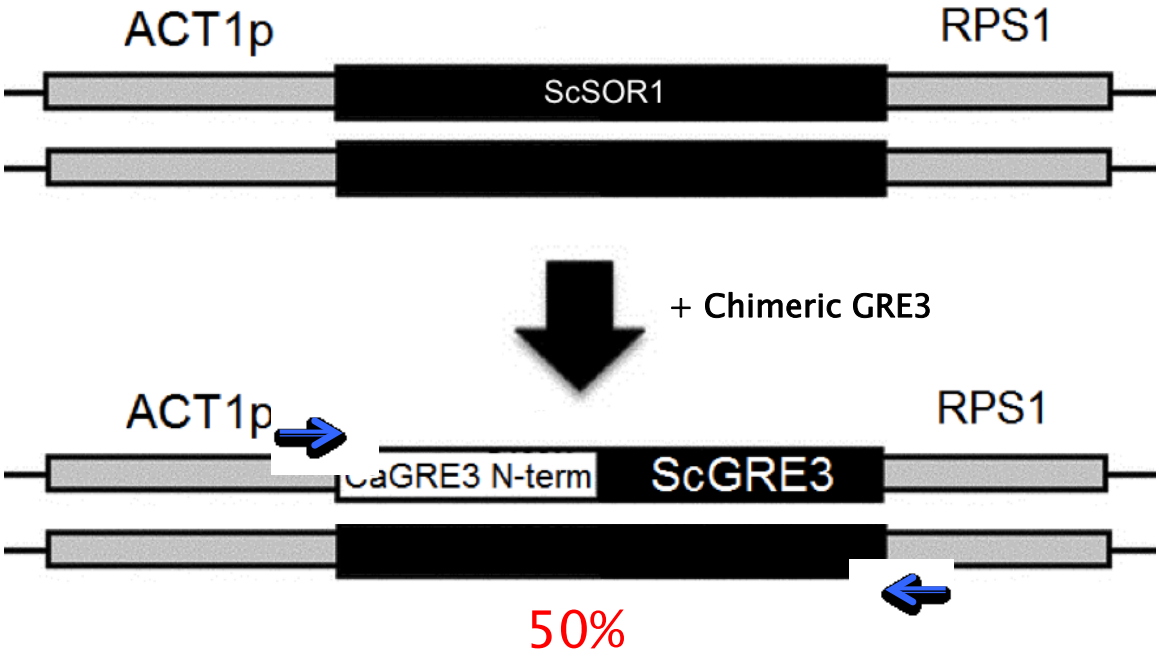

Scenario 2:

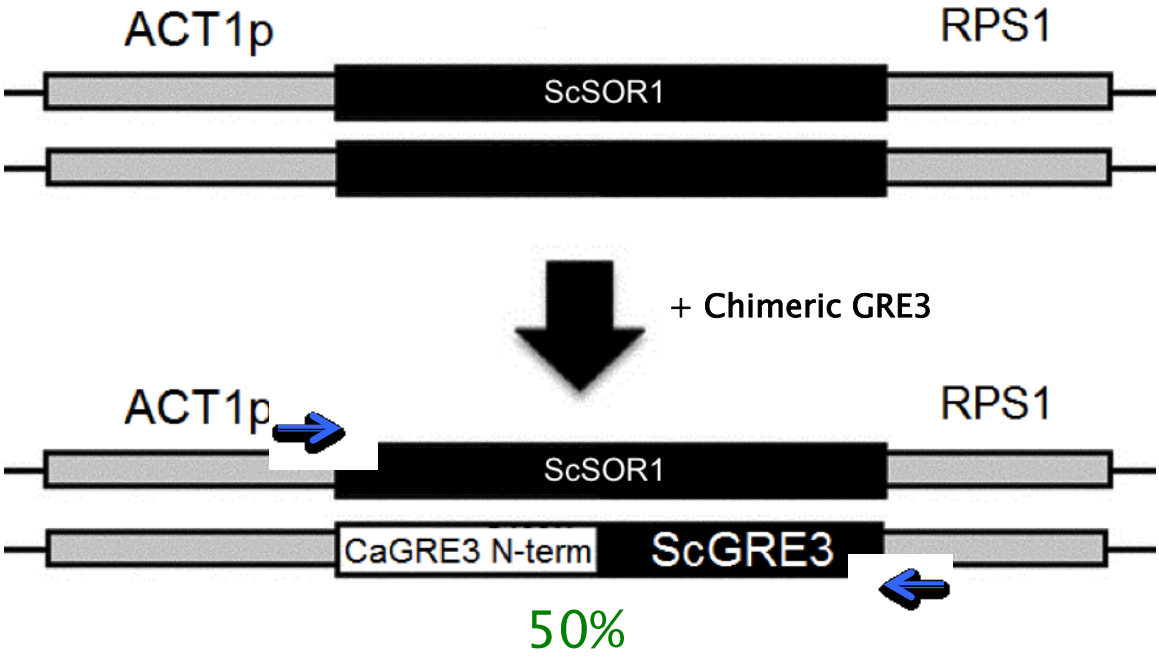

Figure 6D

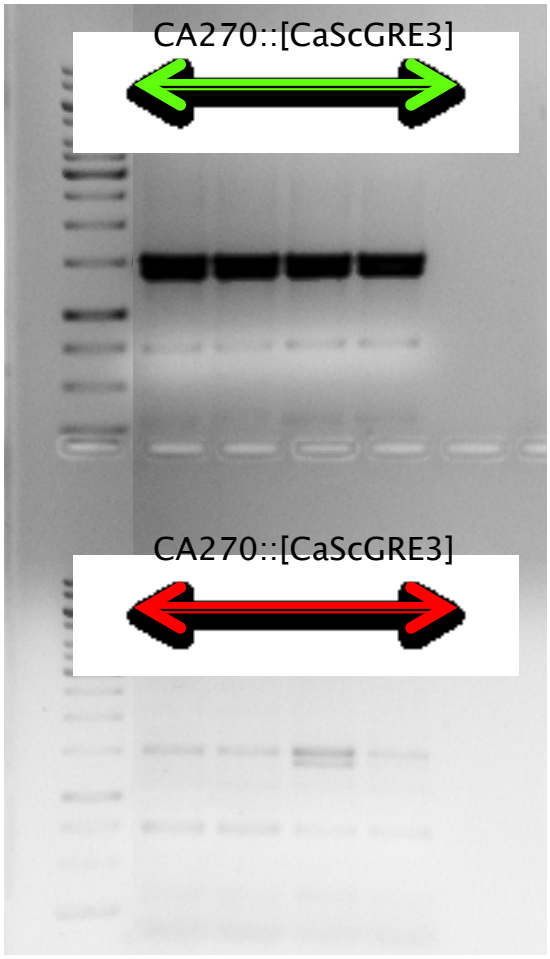

Figure 6E

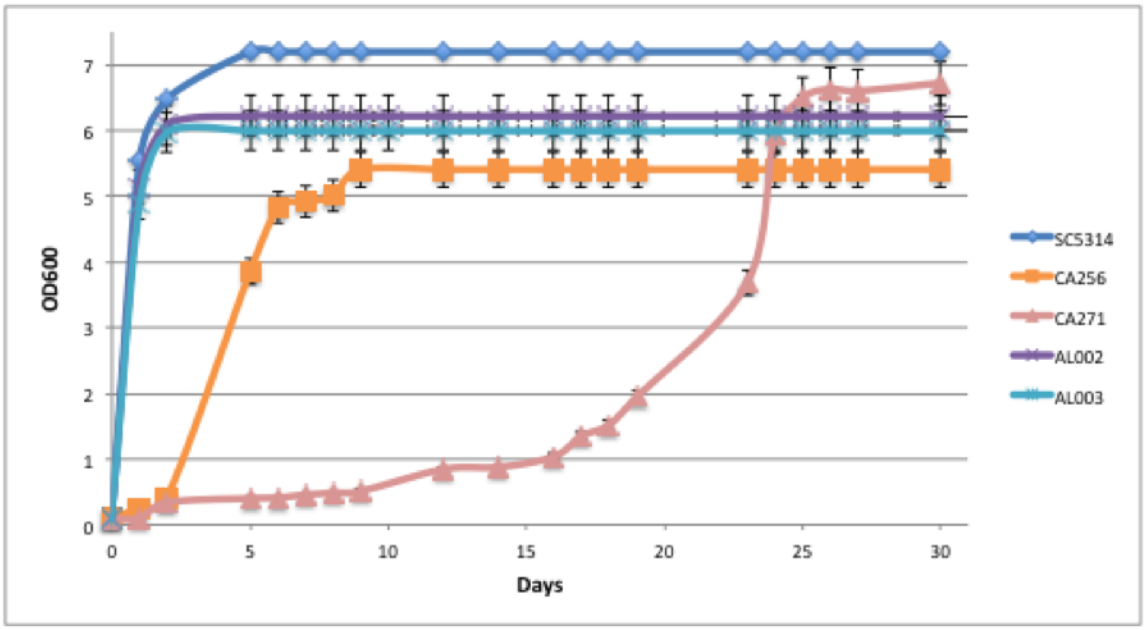
OD600
Days
0
1
2
3
4
5
6
7
0
5
10
15
20
25
30
SC5314
CA256
CA271
AL002
AL003

Figure 7A

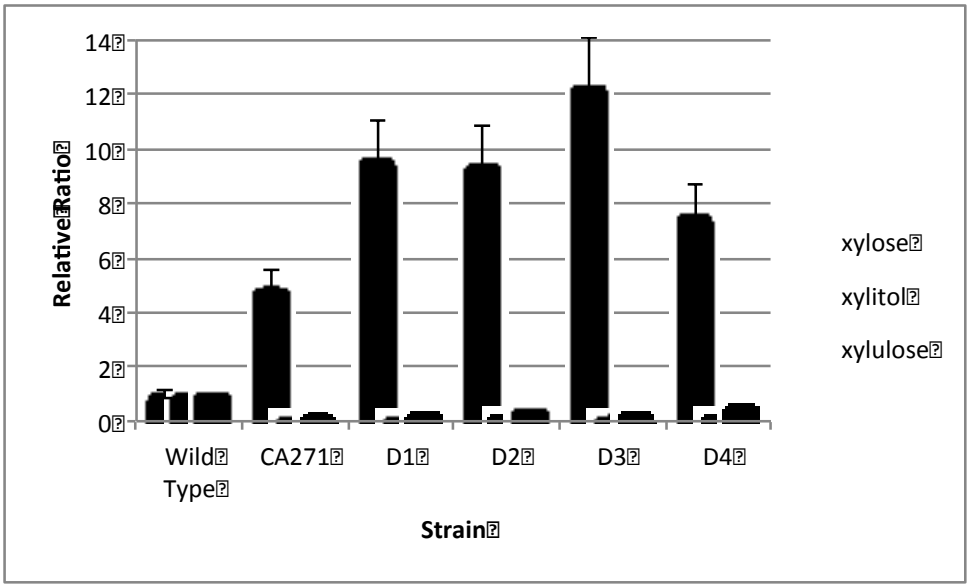
14
12
10
8
6
4
2
0
Relative Ratio
Wild Type
CA271
D1
D2
D3
D4
Strain
xylose
xylitol
xylulose

Figure 7B

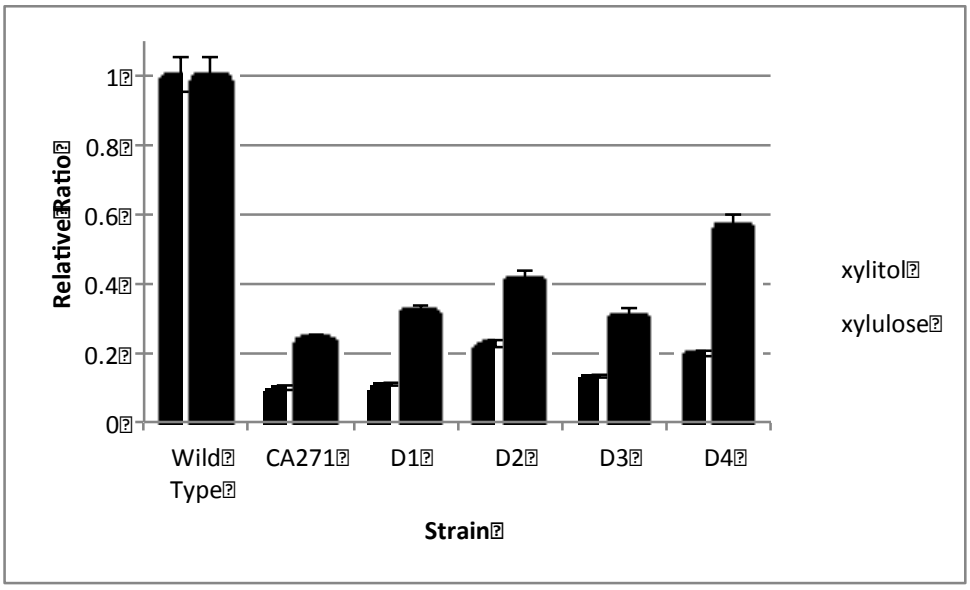
1
0.8
0.6
0.4
0.2
0
Relative Ratio
Wild Type
CA271
D1
D2
D3
D4
Strain
xylitol
xylulose

Figure 8A

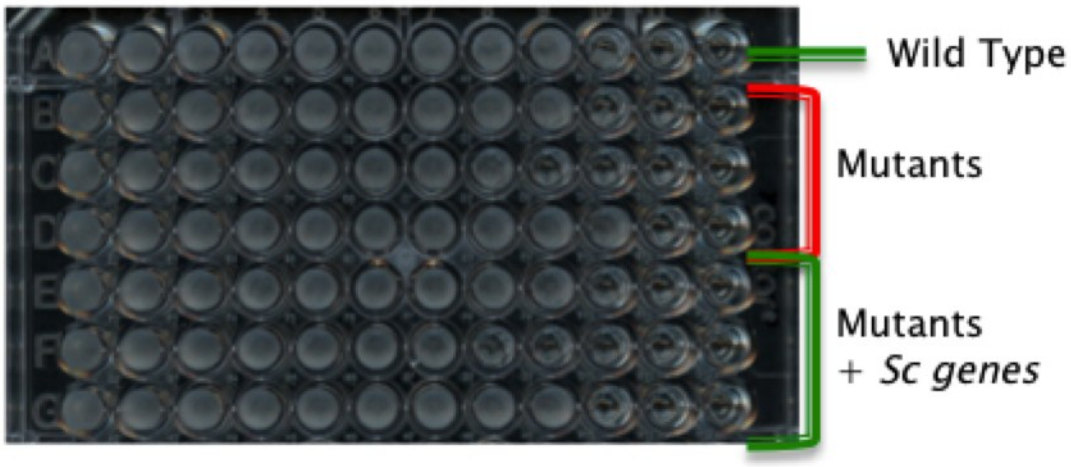

Figure 8B

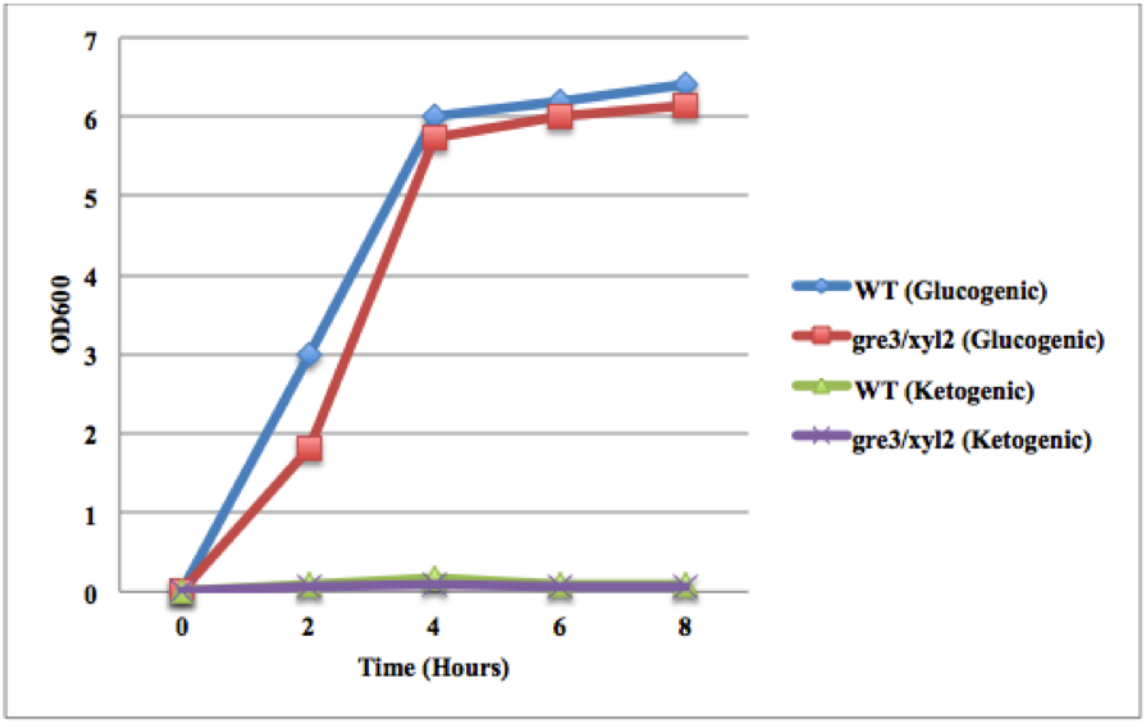
7
6
5
4
3
2
1
0
OD600
0
2
4
6
8
Time (Hours)
WT (Glucogenic)
gre3/xyl2 (Glucogenic)
WT (Ketogenic)
gre3/xyl2 (Ketogenic)

Figure 8C

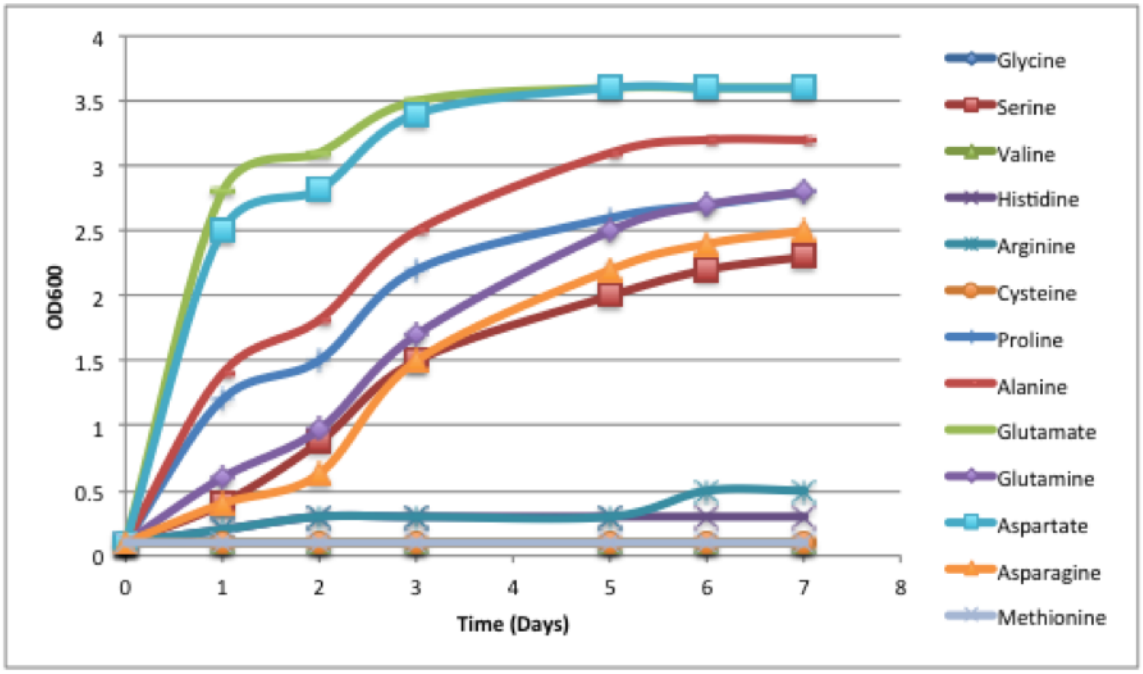
OD600
Time (Days)
0
0.5
1
1.5
2
2.5
3
3.5
4
0
1
2
3
4
5
6
7
8
Glycine
Serine
Valine
Histidine
Arginine
Cysteine
Proline
Alanine
Glutamate
Glutamine
Aspartate
Asparagine
Methionine

Table 1

Table I Plasmids used in this study

Plasmid	Description	Reference
CIpACT-CYC	ACT1p-CYC1t-RPS1-cURA3	Tripathi et al. 2002
pRS314	pBluescript, *TRP1, CEN6, ARSH4*	Sikorski et al. 1989
pl396	CIpACT-CYC with *S. cerevisiae* GRE3 (CTG/Leu to TTG)	Harcus et al. 2013
pAL001	pRS314 with *C. albicans* ACT1p-ScGRE3-RPS1	This study
pAL002	pRS314 with *C. albicans* ACT1p-CaScGRE3-RPS1	This study
pAL003	CIpACT-CYC with *C. albicans* ACT1p-CaScGRE3-RPS1	This study

Table 2

Table II Oligonucleotides used in this study

Oligonucleotide	Sequence	Gene
OAL001	TCCTTTCCTTTCCTTTTCTAATTTTCACTCCTGGTTTTCTTTCTTTCTTAGAAACATTAT CTCGATATTAATATTAAAAAAATATAATCATTCAAAAAGCTTCCTCCCTCTCCCTCCACA	*CaGRE3*
OAL002	ATAAATTTGATTCGCACAGACTTTTTTGTCAATTTTCCAGCACCCTAAGCCGACTAGGGG CATTTTCAAACCGTTATTAAGAGTAACCAATGAAGACATGGTGACTTTCCAACAACCAAA	*CaGRE3*
OAL003	CTCTCCCTCCACACCTTCAT	*CaScGRE3*
OAL004	CAATGCCTCTCTGAGTTGCC	*CaScGRE3*

Table 3

Table III Strains used in this study

Strain	Genotype	Reference
SC5314	Candida albicans wild-type clinical isolate	Gillum et al. 1984
SN148	arg4Δ/arg4Δ leu2Δ/leu2Δ his1Δ/his1Δ ura3Δ::imm434/ura3Δ::imm434 iro1Δ::imm434/iro1Δ::imm434	Noble et al. 2005
gre3	SN148 gre3::HIS3/gre3::ARG4	Harcus et al. 2013
xyl2	SN148 xyl2::HIS3/xyl2::ARG4	Harcus et al. 2013
gre3/xyl2	gre3::HIS1/gre3::ARG4 xyl2::LEU2/xyl2::FRT	Harcus et al. 2013
CDH139	xyl2::HIS1/xyl2::ARG4 RPS1/RPS1:: [CIpACT-CYC *S. cerevisiae* SOR1 (pDH279)]	Harcus et al. 2013
CA256	gre3::HIS1/gre3::ARG4 RPS1/RPS1:: [CIpACT-CYC *S. cerevisiae* GRE3 (CTG/Leu to TTG) (pl396)]	Harcus et al. 2013
CA270	gre3/xyl2 RPS1/RPS1:: [CIpACT-CYC *S. cerevisiae* SOR1 (pDH279)] ura3-/ura3-	This study
CA271	gre3/xyl2 RPS1/RPS1:: [CIpACT-CYC *S. cerevisiae* SOR1 (pDH279)]::[CIpACT-CYC *S. cerevisiae* GRE3 (pl396)]	This study
BY4743	MATa/MATalpha his3Δ1/his3Δ1 leu2Δ0/leu2Δ0 lys2Δ0/LYS2 MET15/met15Δ0 ura3Δ0/ura3Δ0(4741/4742)	Brachmann et al. 1998
W303-1A	MATa ade2-1 canl-100 his3-11,15 leu2-3,112 trpl-l ura3-1	Thomas et al. 1989
AL001	W303-1A:: [pRS314 with *C. albicans* ACT1-CaScGRE3-RPS1 (pAL002)]	This study
AL002	gre3::HIS1/gre3::ARG4 RPS1/RPS1:: [CIpACT-CYC CaScGRE3 (pAL003)]	This study
AL003	gre3/xyl2 RPS1/RPS1:: [CIpACT-CYC *S. cerevisiae* SOR1 (pDH279)]::[CIpACT-CYC CaScGRE3 (pAL003)]	This study

Supplementary 1: Glucogenic Amino Acids Growth Chart

Amino Acid	Enzyme Involved	Gene in *C. albicans*	End Product
L-Serine	Dehydratase (1)	ILV1	Pyruvate
L-Cysteine	Transaminase (2)	None	Pyruvate
L-Alanine	Transaminase (1)	ALT1	Pyruvate
L-Histidine	Ammonia Lyase (4)	None	L-Glutamate
L-Aspartate	Ammonia Lyase (1)	None	Fumarate
L-Aspartate	Transaminase (1)	AAT21	Oxaloacetate
L-Asparagine	Asparaginase (1)	orf19.7593	L-Aspartate
L-Glutamate	Dehydrogenase (1)	GDH2	α-Ketoglutarate
L-Glutamine	Glutaminase (1)	HIS7, SNO1, SNZ1	L-Glutamate
L-Proline	Pyrroline-5-carboxylate reductase (2)	PRO3	L-Glutamate
L-Methionine	Methyl-Malonyl-CoA Mutase (9)	None	Succinyl-CoA
L-Valine	Methyl-Malonyl-CoA Mutase (10)	None	Succinyl-CoA
L-Arginine	Various (3)	CAR1, CAR2, PRO2	L-Glutamate
L-Glycine	Serine HydroxyMethylTransferase (2)	SHM1	Pyruvate

Grows (has necessary enzymes)

Does not grow (lacks necessary enzymes)

Does not grow (but has necessary enzymes)

Supplementary 2: pAL001 Plasmid Map

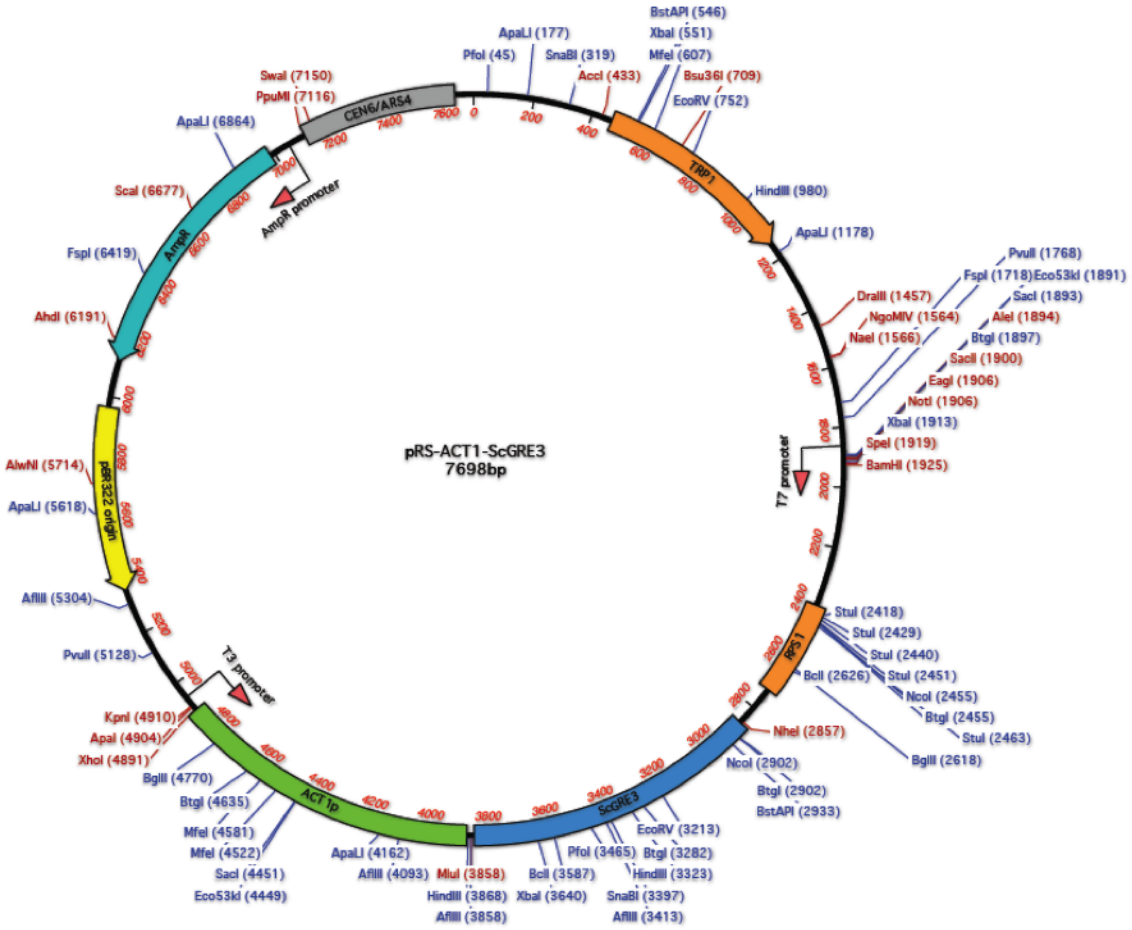

Supplementary 3: pAL002 Plasmid Map

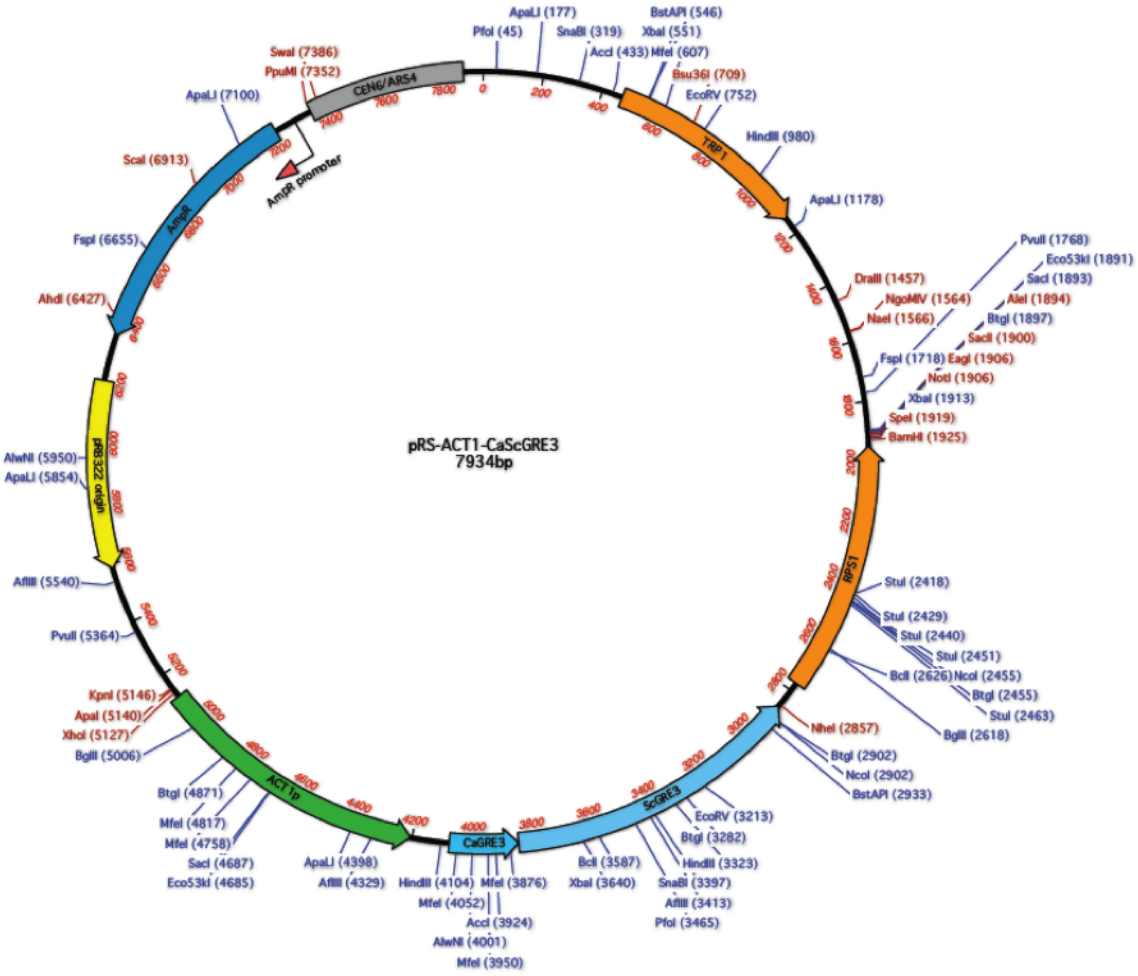

Supplementary 4: pAL003 Plasmid Map

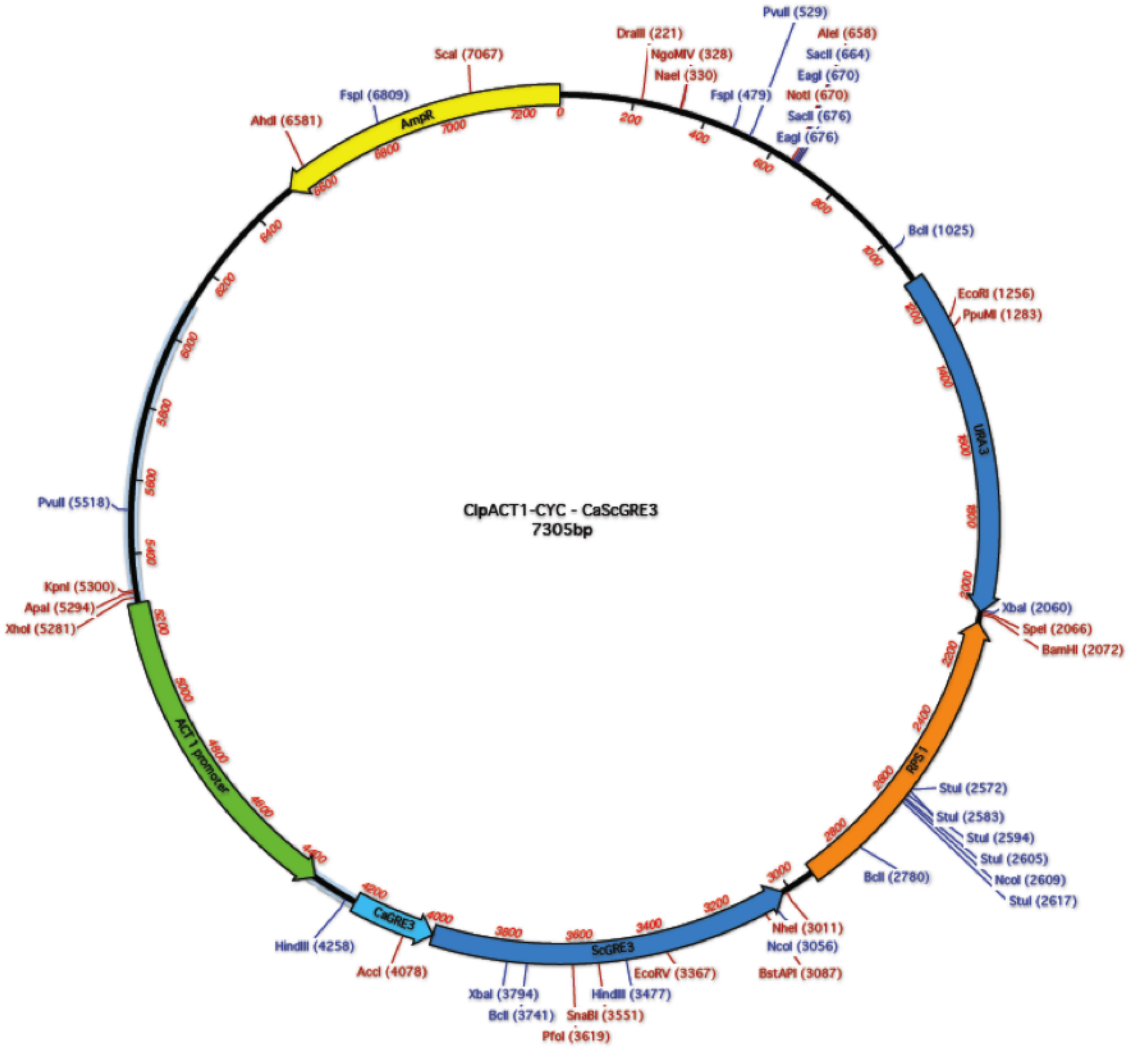

Supplementary 5: Adapted-Evolution Growth Assay Conditions

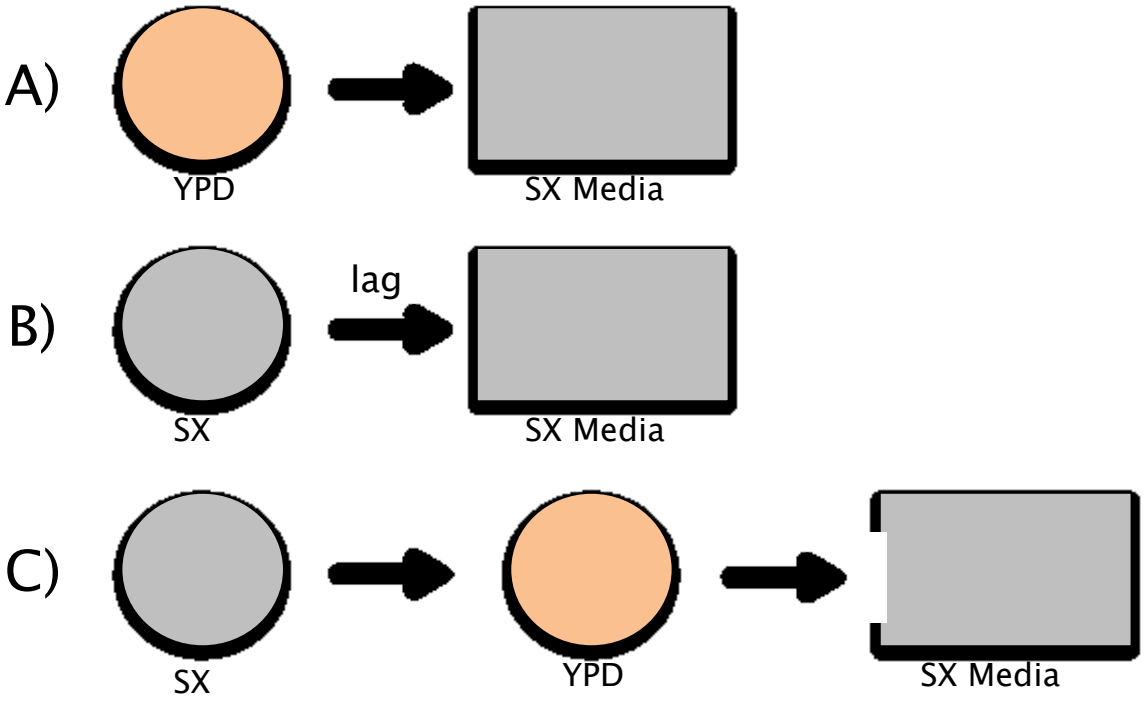

Supplementary 6: Adapted-Evolution Growth Assay (Day 5)